國 立 交 通 大 學

生物科技學系

碩 士 論 文

探討乙醯膽鹼酯酶在固定化和游離狀態下之酵素動力學

Kinetics of Free and Immobilized *Acetylcholinesterase*

研究生：李奇叡

指導教授：楊裕雄 教授

中華民國一百零一年五月

探討乙醯膽鹼酯酶在固定化和游離狀態下之酵素動力學

Kinetics of Free and Immobilized *Acetylcholinesterase*

研究生：李奇叡　　Student: Chi-Ruei Lee
指導教授：楊裕雄　　Advisor: Yuh-Shyong Yang

國立交通大學
生物科技學系
碩士論文

A Thesis
Submitted to Department of Biological Science and Technology
National Chiao Tung University
in Partial Fulfillment of the Requirements
for the Degree of
Master of Science
in
Biological Science and Technology
May 2012
Hsinchu, Taiwan, Republic of China

中華民國一百零一年五月

探討乙醯膽鹼酯酶在固定化和游離狀態下之酵素動力學

學生：李奇叡　　指導教授：楊裕雄 教授

國立交通大學生物科技學系碩士班

摘要

在過去的文獻中，關於乙醯膽鹼酯酶(E.C. 3.1.1.7)的研究，大多是探討在游離狀態下的酵素特性變化。但是在生物體中乙醯膽鹼酯胺並不是以游離的狀態存在，而是以鑲嵌的方式固定在細胞膜上，因此酵素的特性可能在不同的生理條件下而有差異。本研究將乙醯膽鹼酯酶固定在二氧化矽晶片上以模擬此酵素固定在細胞膜上的環境。配合實驗室之前開發的量測固定化酵素平台，測量出被固定化的乙醯膽鹼酯酶的酵素動力學參數 K^*_m 和 V^*_{max}，探討三維和二維的乙醯膽鹼酯酶在兩種不同狀態下的酵素動力學。本研究利用 LabVIEW 圖形化程式將固定化酵素量測平台過於繁雜的分析過程，開發為自動化計算的人機介面。此程式縮短了繁瑣的計算程序同時在短時間內就能得到固定化酵素的動力學參數 K^*_m 和 V^*_{max}。 整合此兩套系統將能夠快速得到研究所需要之固定化酵素動力學參數。乙醯膽鹼酯酶在二維狀態下酵素動力學參數 K^*_m 為 46±3 μM 和 V^*_{max} 為 7.2±0.6 μmole/mg/min；而三維狀態下酵素動力學參數 K_m 為 79±8 μM 和 V_{max} 為 159±5 μmole/mg/min。目前治療阿茲海默症的主要方法為，利用藥物抑制乙醯膽鹼酯胺進而減少神經傳遞素，以減緩此症狀的發生，未來本技術將可應用於探討藥物抑制乙醯膽鹼酯酶的活性。

Kinetics of Free and Immobilized *Acetylcholinesterase*

Student: Chi-Ruei Lee Advisor: Prof. Yuh-Shyong Yang

Department of Biological Science and Technology

National Chiao Tung University

ABSTRACT

Enzymatic properties of *acetylcholinesterase* (AChE, E.C. 3.1.1.7) were mainly studied in vitro at it free form in solution. However, the *in vitro* properties of the enzyme may differ in physiological condition because AChE is immobilized as a membrane anchored protein in the organism. The method of this research was to immobilize AChE on silicon oxide surface in order to imitate the virtual environment of the cell membrane. Based on a measurement platform previously developed by our laboratory, K^*_m and V^*_{max} of immobilized AChE on planar silicon surface were determined. Automatic LabVIEW graphical program were developed to replace previously complicated analyzing processes, meanwhile, generated the kinetic parameters of immobilized enzyme. Kinetic parameters, K_m and V_{max}, of AChE were 46±3 μM and 7.2±0.6 μmole/mg/min in two dimension (on silicon oxide surface) and 79±8 μM and 159±5 μmole/mg/min in three dimension (in solution), respectively. Nowadays, controlling AChE activity by medicine to reduce acetylcholine is the main solution for treating Alzheimer's disease. This technique can be used for investigating immobilized AChE activity under the influence of inhibitors that can be applied to the treatment of Alzheimer's disease.

Acknowledgement

轉眼間，三年的黃金歲月一下子就消逝了，很感謝楊裕雄教授提供了一個如此自由的研究環境、充沛的研究資金和培養我獨立思考的研究精神。這所有的一切是我由衷所感謝的。在此也特別感謝柯富祥教授、徐琅教授能夠抽空參加我的碩士口試，給予我許多研究方面的寶貴意見，讓我受益良多。

短暫的三年，很高興認識了 LEPE 這個大家庭，從我一開始進來一起同甘共苦的曉萍、芝綺，很開心你們提早了開始你們人生中另一段的旅程，而我也終於可以走向另一個人生階段，祝福你們!此外，也很感謝實驗室的大老們，陸宜學長、程允學長、普普學長、胖哥、晨竹、咏馨、康寧、文燦、還有各位學弟妹們，謝謝你們陪我度過了過去難熬的歲月。在這裡也特別感謝小志學長在我實驗上有困難的時候，總是讓我從困境中抽身而出，在我低潮時，會陪我一起打球紓解壓力。另外也要恭喜你拿到博士學位，等待六年是值得的!經歷了有淚有笑的三年時光，終於拿到了碩士學位，始終最感謝的還是蘇博，不管在研究態度、做人處理上、讓我學到了許多寶貴的人生經驗。每當遇到困難和低潮時，你總是以正面的角度鼓勵我，讓我遠離負面的情緒，也會告訴我"唯有面對問題，才能夠真正解決問題"。曾經你說過得那些話，我會永遠記得，謝謝你!

最後還是謝謝我親愛的家人們。毛、老爸、老媽、老姐、和老哥和未來的大嫂，感謝你們一路上的支持和陪伴，無怨無悔得在我背後支持著我。我能夠拿到這個學位，有一半是你們的功勞，謝謝你們!相信在經歷過這段歷練後，未來沒有什麼事情是不可能。最後送上喬丹名言，大家共勉之:

I can accept failure ,but I can't accept not trying!

奇叡

2012.5

Contents

PAGE

Contents of Tables PAGE

Contents of Figures PAGE

Abbreviation

Abbreviation	Full Name
AChE	*acetylcholinesterase*
ATChI	acetylthiocholine iodide
DTNB	5,5-dithiobis-(2-nitrobenzoic acid)
TNB	2-nitro-5-thiobenzoic acid
K-PB	potassium phosphate buffer
APTES	3-triethoxysilylpropylamine
AD	Alzheimer's disease

I Introduction

1-1 Introduction of *acetylcholinesterase*

Acetylcholinesterase (AChE, E.C. 3.1.1.7), also known as AChE , is a tetramer composed of 4 equal subunits of 70 kDa each. It's a glycoprotein that exists is several forms and the membrane-bound globular AChE forms have hydrophobic domains that anchor them in the membrane phospholipid bilayers [1]. This is an evolutionary consequence of one of its key active hydrolysis of the neurotransmitter acetylcholine (ACh) to terminate signaling in cholinergic synapses, including the neuromuscular junction, so the great speed of the enzyme is essential for rapid modulation of synaptic activity (Figure 1). In the other hand, *Acetylcholinesterase* also plays an important role in cholinergic transmission by catalyzing the rapid hydrolysis of the neurotransmitter acetylcholine (ACh) into acetate and choline [2]. Moreover, *acetylcholinesterase* is also found on other tissue like the red blood cell, muscle, heart.

1-2 Introduction of Alzheimer's disease

Alzheimer's disease (AD) is one of slowly progressive disease of the brain that is characterized by impairment of memory and eventually by disturbances in reasoning, planning, language, and perception [3, 4]. In many research, they think that Alzheimer's disease results from an increase in the production or accumulation of a specific protein (β-amyloid protein) which is in the brain that leads to nerve cell death [5]. Moreover, many of research find out more about the causes of Alzheimer disease until now there is no one reason why people get Alzheimer disease. At present, researchers find older people are more likely to get it, and the risk gets greater the older the person gets. For instance, the risk is higher for someone who is 85 years old than it is for someone who is 65. And women are more likely to get it than men [6]. Researchers also think genes handed down from family members can make a person more likely to get Alzheimer disease. But that doesn't mean everyone related to someone who has Alzheimer disease will get the disease [7]. Other factors, combined with genes, may make it more likely that someone will get the disease. Although AD can't be cured and is degenerative but we can prevent it from risk factor like high blood pressure, high cholesterol, down syndrome, or having a head injury. Keeping the positive side that researchers believe exercise, a healthy diet, and taking steps to keep your mind active may help delay the onset of Alzheimer disease [8].

1-2.1 Symptoms of Alzheimer's disease

Alzheimer disease can affect people in many ways, but the most common symptom pattern is gradually worsening difficulty in remembering new information because disruption of brain cell function usually begins in regions involved in forming new memories [9-11]. When damage spreads, individuals experience as the following are warning signs of AD:

•Memory loss that disrupts daily life.

•Challenges in planning or solving problems.

•Difficulty completing familiar tasks at home, at work, or at leisure.

•Confusion with time or place.

•Trouble understanding visual images and spatial relationships.

•New problems with words in speaking or writing.

•Misplacing things and losing the ability to retrace steps.

•Decreased or poor judgment.

•Withdrawal from work or social activities.

•Changes in mood and personality.

1-2.2 Deaths from Alzheimer's disease

Nowadays, AD is becoming a more common cause of death as the populations of the United States and other countries age [12-15]. Even though other major causes of death continue to experience significant declines, those from AD have continued to rise. Between 2000 and 2008 (preliminary data), deaths attributed to AD increased by 66%, whereas those attributed to the number one cause of death, heart disease, decreased by 13% as shown in Figure 2.

The increase in the number and proportion of death certificates listing AD reflects both changes in patterns of reporting deaths on death certificates over time as well as an increase in the actual number of deaths attributable to AD [16-19]. Severe dementia frequently causes complications such as immobility, swallowing disorders, and malnutrition [20, 21]. These complications can significantly increase the risk of developing pneumonia, which has been found in several studies to be the most commonly identified cause of death among elderly people with AD and other dementias. The situation has been described as a "blurred distinction between death with dementia and death from dementia". Regardless of the cause of death, 61% of people with AD at the age of 70 are expected to die before the age of 80 as compared with 30% of people at the age of 70 without AD [18].

1-3 Motivation

In past research, deaths attributed to Alzheimer's disease increased by 66% that means Alzheimer's disease become a serious problem in the 21st century . According to curing Alzheimer's disease related with enzymatic kinetics of AChE in past report so that we selected this important enzyme for research [22-27]. Soluble AChE was already used to study its biological properties and pharmaceutical products in the past but it might not be a suitable approach to investigate AChE in real situation [28-31]. Thus, it become very important to be able to determine the kinetics of enzyme immobilized on the planar surfaces within the microfluidic system in order to evaluating the function of the whole system. So far, there is no such method reported. In past research, our lab developed a novel kinetic model, based on systematized and standardized approach, for measuring K^*_m and V^*_{max} of enzyme immobilized on planar silicon oxide surface within a microfluidic bioreactor [32] In this study, we further developed the novel kinetic model into automatic program, which was designed by software of LabVIEW. Then, we could easily get parameters of apparent K^*_m and V^*_{max} as soon as we used automatic program. Finally, we could compare enzymatic kinetics of immobilized and soluble enzyme with two kind of kinetic model.

II Material and method

2-1 Experimental material

1. **Compound : *Acetylcholinesterase* (AChE)-type V-S from Electric eel**

   Company: Sigma-Aldrich

   Molecular weight: 280 kDa

   Assay: ≥ 60%

2. **Compound : Acetylthiocholine iodide (ATChI)**

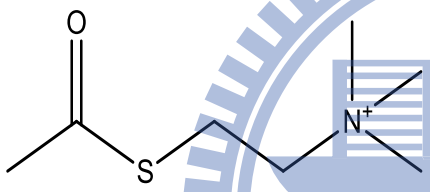

   Company: Sigma-Aldrich

   Molecular weight: 289.18

   Soluble in DI water

3. **Compound : 5,5-dithiobis-(2-nitrobenzoic acid) (DTNB)**

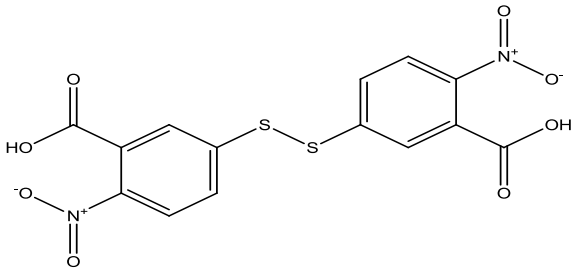

   Company: Sigma-Aldrich

   Molecular weight: 289.18

   Soluble in ethanol

4. **Compound: Potassium phosphate monobasic (KH_2PO_4)**

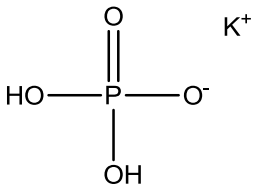

Company: Sigma-Aldrich

Molecular weight: 136.09

5. **Compound: Potassium phosphate dibasic (K_2HPO_4)**

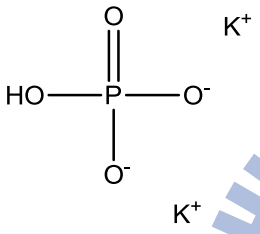

Company: Sigma-Aldrich

Molecular weight: 174.18

6. **Compound: Ethanol (CH_3CH_2OH)**

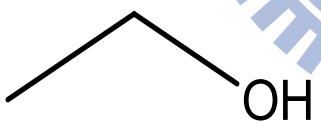

Company: Echo Chemical Co.

Molecular weight: 46.07

Assay: 99.5%

7. **Compound: (3-Aminopropyl)triethoxysilane (APTES), $H_2N(CH_2)_3Si(OC_2H_5)_3$**

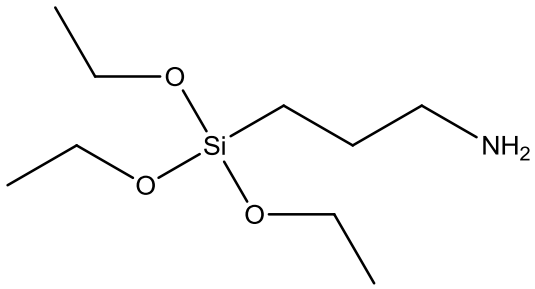

Company: Sigma-Aldrich.

Molecular weight: 221.37

Assay: 98%

Soluble in ethanol

8. **Compound: Glutaraldehyde solution, $(CH_2(CH_2CHO)_2)$**

Company: Fluka (USA)

Molecular weight: 100.12

Assay: ~25% in H_2O

9. **Compound: Sulfuric acid, (H_2SO_4)**

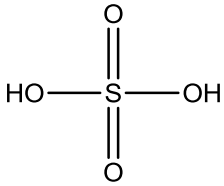

Company: Sigma-Aldrich.

Molecular weight: 98.08

Assay: 99.9%

10. Compound: Hydrogen peroxide solution, (H_2O_2)

Company: Sigma-Aldrich.

Molecular weight: 34.01

Assay: 30%

11. Phosphate buffer (PB) was prepared in deionized (DI) water and its pH was adjusted to 8 .

12. Deionized and distilled water (DI water, ddH_2O)

The water we used was purified with filters, reverse osmosis, and deionized system until the resistance was more than 18 MΩ·*cm*. DI water was used to clean, wash, and be a solvent.

13. P-type Si(100) wafers (14-21 Ω-cm, MEMC, MO, USA)

It is 15 cm diameter, on which 100 nm oxide layers were grown using wet oxidation with a gas mixture of hydrogen (8000 cm^3/min) and oxygen (5000 cm^3/min) at 978^oC.

2-2 Instruments

1. NI LabVIEW 2011

It is a comprehensive development environment that provides engineers and scientists unprecedented hardware integration and wide-ranging compatibility. On the other hands, it is also a program used to automate testing and data gathering. It is basically a graphical programming language in which the user can set up the program to manipulate and store data.

2. UV–Vis spectroscopy (HITACHI, U-3310, Tokyo, Japan)

UV–Vis uses light in the range of near UV, visible and near infrared. The absorption in the light range is due to the optical properties of the chemicals involved.

3. Programmable syringe pump (KD Scientific, KDS260P, USA)

We utilized programmable syringe pump to translate reaction solution into the channel and eluted to a spectrophotometer for the determination of the concentration of reporter molecules.

4. Hot plate (SHIN KWANG)

After the patterned sample of interest was immersed in the APTES solution for 30 min in room temperature we banked the patterned sample at 120^{o}C for 30 min.

5. X-ray photoelectron spectroscopy (XPS)

It was used to verify the attachment of the AChE onto the surfaces of the silicon.

2-3 Experiment procedures

2-3.1 Silica pattern formation processes

P-type Si(100) wafers (14-21 Ω-cm, MEMC, MO, USA) with 15 cm diameter were deposited and etched to form the structure with silicon oxide pattern on poly-Si film. To prepare the silicon oxide pattern on poly-Si film, the poly-Si film was first deposited with silane gas (SiH_4) at 60 cm^3/min and 620^oC. Prior to photolithography, the silicon oxide film was grown by wet oxidation with a gas mixture of hydrogen (8000 cm^3/min) and oxygen (5000 cm^3/min) at 978^oC. The mask with the pattern of interest was used to define the photoresist (TMER-iP3650, Tokyo Ohka Kogyo, Tokyo, Japan) pattern. A 365 nm light emitted from high pressure mercury lamp (SUV-2001CIL, USHIO, Tokyo, Japan) induced the photo-active reaction for the photoresist film. After the dissolution of exposure area with 2.38% tetramethylammonium hydroxide, the plasma was used to etch the silicon oxide film without passivation by photoresist pattern. The reactive-ion etch system (TE5000, Tokyo Electron Limited, Tokyo, Japan) was operated at 500W RF power under 0.2 Torr high vacuum, and the gas mixture of 20 cm^3/min of CF_4, 20 cm^3/min of CHF_3, and 400 cm^3/min Ar. Finally, the residual photoresist was removed and cleaned by the mixing chemical of H_2SO_4 and H_2O_2 (volume ratio = 3:1) at 120^oC for 10 min. The chemicals used were of higher grade from Merck (Darmstadt, Germany).

2-3.2 Immobilization of *acetylcholinesterase* on surface silicon wafer

In order to immobilization, the piece of silicon oxide wafer would be clean carefully by the SPM solution (sulfuric-peroxide mixture), H_2SO_4 and H_2O_2 (volume ratio is 3:1) twice and incubated the temperature at 120°C for 30 min. It should be noted that the cleaning solution is very corrosive and dangerous. After rinsing with pure water and drying, the sample was immersed in the (3-aminopropyl)triethoxysilane (APTES, Sigma–Aldrich, MO, USA) solution to proceed the silanization reaction for 30 min at room temperature to create an amine-functional surface. The APTES solution was prepared by the following procedures: preparing the 5% APTES solution by diluting with 95% ethanol. Following the APTES treatment, the silicon wafer was rinsed with 95% ethanol thoroughly. Then, the silicon wafer was baked at 120°C for 30 min to complete the Si–O bond formation. The sample was immersed in the linker solution (12.5% glutaraldehyde, i.e. pentane-1,5-dial) for 60 minutes in room temperature. The 12.5% glutaraldehyde solution was diluted with DI water (deionized system until the resistance was more than 18 MΩ·*cm*) from 25% glutaraldehyde (in water, Sigma-Aldrich)[34]. Finally, the patterned sample was immersed in the

((AChE)-type V-S from Electric eel (Sigma-Aldrich)) solution that the powder of *acetylcholinesterase* (AChE) was dissolved in phosphate buffer (PB buffer, pH 8)) for 30 minutes at room temperature. Then, we washed patterned sample by PB buffer and dried with nitrogen gas. The overall surface modification is shown in Figure 3.

2-3.3 Enzyme standard assay of soluble AChE

In this research, AChE activity of both soluble and immobilized enzyme was determined according to the Ellman method (See Figure 4). In determination of soluble AChE activity, the reaction solution was prepared by mixing PB solution (pH 8.0, 10 mM), various concentration of acetylthiocholine iodide, 0.1 mM DTNB and added an appropriate amount of the enzyme [31, 35-37]. After mixing the catalytic substance with the reactants, the initial product release at the onset of the reaction was measured using a personal computer and a Hitachi UV–Vis-3310 enzyme reaction measurement system (a UV–Vis spectrophotometer possessing a temperature-controlled thermostatted cell holder; Hitachi, Tokyo, Japan). For the soluble AChE kinetics analysis, the initial reaction of the change in absorbance at 410 nm was recorded (in real-time). The initial rate of the absorption change against the reaction time was converted to enzyme activity using a molar absorption coefficient of 13600 M^{-1} cm^{-1} for the product of 2-nitro-5-thiobenzoic acid (TNB). The values of

K_m and V_{max} were obtained through nonlinear regression analysis using SigmaPlot 2001 (v. 7.0) and Enzyme Kinetics Module (v. 1.1, SPSS, Chicago, IL USA) software. The assays were obtained in triplicate; average values were reported. All activity assay experiments were carried out at room temperature.

2-3.4 Enzyme standard assay of immobilized AChE and reactor system

Preliminary tests for the immobilization of AChE activity were carried out using home-made apparatus and checked activity with Ellman's method. The home-made apparatus (Figure 5) was designed and used to evaluate the enzyme activity on the sample surface of interest. The Teflon ring tightly contacted with the substrate and sealed with the silicon resin glue. Prior to conducting the enzyme immobilization, we needed to test the reliability of the home-made apparatus to avoid leakage problem. The clean and APTES immobilization methods for enzyme immobilization were conducted in the home-made apparatus with the same procedures as mentioned above. The sample was repeatedly immersed by fresh 10 mM potassium phosphate buffer for five times to wash away the residual enzyme solution. Observation of the activity of the enzyme was a direct method to know whether the enzyme was successfully immobilized or not. The reaction solution was prepared by adding the 1 mM acetylthiocholine iodide (ATChI), 0.1 mM 5,5-dithiobis-(2-nitrobenzoicacid) (DTNB)

into the solvent of 10 mM potassium phosphate buffer (PB) at pH 8. Then, we added the above solution into the home-made apparatus. At the reaction time of interest, the liquid was siphoned out from the home-made apparatus to an UV-Vis spectrophotometer (Hitachi UV-Vis-3300, Tokyo, Japan) for characterization. We analyzed the absorbance of 2-nitro-5-thiobenzoic acid (the catalytic product of 5,5-dithiobis-(2-nitrobenzoicacid)) at 410 nm wavelength to determine the activity of *acetylcholinesterase*. After we know the enzyme successfully was immobilized onto surface, we could study further enzyme kinetics assay of immobilized AChE with home-made micro- fluidic reactor system further. According to the model which have been published by our lab [32] that we have constructed a novel home-made micro-fluidic system (Figure 6) for assay enzymatic kinetics parameter of immobilized enzyme.

This novel bioreactor design has a flow channel, which is made of glass and the reaction liquid filled in cylinder is continuously pushed by syringe pump. To utilize this micro-fluidic reactor system for measuring enzymatic kinetics parameter of immobilized enzyme has two parts. For first part, we should construct baseline in order to confirm the reaction liquid is stable and unchanging with time. In baseline, the reaction liquid would not go through flow channel, it only goes through cuvette and detect its absorbance via UV-Vis spectrophotometer without enzymatic catalysis.

For second part, the reaction liquid also would continuously go through flow channel and the reaction liquid is simultaneously catalyzed by immobilized enzyme. Finally, the product of reaction liquid flow through cuvette and detect its absorbance by UV-Vis spectrophotometer. In experiment, two different concentrations of acetylthiocholine iodide (ATChI), 1000 μM and 50 μM, were used to create saturating and non-saturating substrate condition, respectively, for the immobilized AChE-catalyzed reaction with home-made micro-fluidic reactor system. The ATChI concentrations used were determined according to the K_m of free *Acetylcholinesterase* from Electrophorus electricus and the reaction mixtures for immobilized AChE contained ATChI (1000 μM or 50 μM) and 0.1 mM DTNB in 10 mM potassium phosphate buffer at pH 8. Injection of the reaction mixtures into the reactor was controlled by automatic pumping system and operated at desired to have space time (τ) at 0.5 min, 1 min, 2 min. The output solution was directed into a quartz flow cell mounted in the UV-Vis spectrophotometer (Hitachi UV-Vis-3300, Tokyo, Japan) for TNB detection at 410 nm. The results of immobilized kinetics experiments were analyzed by theoretical considerations (as shown in appendix I.) that was constructed by our lab. All of analysis data used represent mean value derived from three determinations.

2-4 Development of theoretical model to analytic program based on LabVIEW

Theoretical model previously developed [32] fits very well to the kinetics of immobilized enzyme on one-side planar surface (detailed analysis and prediction of kinetics are given in Appendix I). Unfortunately, this theoretical model was too complicated to utilize and difficult for further development for automation. According to process of model, we utilized software of LabVIEW to develop the analysis program divided into three parts. Therefore, it could easily get the kinetic parameters of immobilized enzyme as soon as possible by operating the analysis program. In the first part of the analysis program, we need to modify the raw data of progress curves of immobilized-enzyme reaction cycles. Hence we set some required parameters such as flow rate (μl/min), space time (min), extinction coefficient of product (ε) and high/low feed concentration of substrate (μM) (Figure 8 (a)). Next, we use LabVIEW to fit the data points of high/low baseline concentration to get the background during the experiments (Figure 8 (b)). Then, the reaction data at high/low concentration will be modified by the fitting curve through the "modify" button based on the analysis program. (Figure 8 (c)). In the second part, we modified reaction data at high/low concentration to calculate of the kinetic parameters. After successively first computing, we will get the initial approximation of $<\frac{V^*_{\max}}{H}>_0$, $<K^*_m>_0$ and decay

curve about the issue of deactivation of immobilized enzyme (Figure 9). Finally, we key the modified reaction data at high/low concentration into the third part of the analysis program. By initial $< K_m^* >_0$ and these modified will get the final approximation of $< \frac{V_{\max}^*}{H} >_r$, $< K_m^* >_r$ and decay curve (Figure 10).

III Results and discussion

3-1 Determining the surface modification of silicon wafer for immobilization enzyme

In this experiment, we dropped the *acetylcholinesterase* solution onto a silicon wafer modified with functional linker for three main steps (Figure 3). Every immobilized step was following standard flowchart and then we checked each immobilized step for percentage of elemental analysis that was characterized by X-ray photoelectron spectroscopy (XPS) (See Figure 11).

The XPS was used to verify the attachment of the enzymes onto the surfaces of the functional linker (See Table 1). For the cleaning silicon wafer without surface modification, the total percentage of elemental analysis indicates that the percentage of N_{1s} approaches zero. The result implies there is no pollution onto surface. In second immobilized step, we dropped some 5% APTES solution on surface of silicon wafer. The result points out the percentage of N_{1s} increases about 10%, it means APTES reacts with the surface silanol group (Si-OH) to form primary amine group on silicon dioxide film. In third immobilized step, 25% glutaraldehyde is subsequently used to react with the surface amine group. Owing to yielding an imine linkage (C=N) with one end aldehyde group in glutaraldehyde so that we can see the percentage of N_{1s} decreases to 5%. At last, we subsequently loaded *acetylcholinesterase* (AChE)

solution to react with surface aldehyde group. The result shows the percentage of C_{1s} elevates to 66%. All of result are in agreement with the existing literature for proteins and enzymes bound to the surface of silicon wafer with surface modification.

3-2 Confirm activity of surface-immobilized AChE

It is obvious that the surface of silicon nitride and poly-Si have no active group for immobilization. The bio-important enzyme, i.e. AChE, can be assembled onto the silicon dioxide film. The reaction having three main steps is illustrated in Figure 3. Hence, the AChE is successfully immobilized onto the surface of silicon oxide film. The analysis of surface enzyme (AChE) activity is very complex [36, 38]. Figure 12 shows the time course of the changes in Ultraviolet-visible for the assay reaction and corresponding controls, where specific components that of the reaction mixture were omitted. Only complete reaction was observed an increase of absorption at 410 nm, reflecting the enzyme activity of AChE (Figure 12).

Figure 4 illustrates the two simultaneous chemical reactions appeared in the home-made apparatus (Figure 5). The acetylthiocholines iodide (ATChI) is transferred into the thiocholine molecule under the catalysis by the AChE enzyme and translated with 5,5-dithiobis-(2-nitrobenzoic acid) (DTNB) to yielding the products of 2-nitro-5-thiobenzoic acid (TNB). Once the enzyme is still active, the concentration of TNB is gradually accumulation. Therefore, the absorbance at 410 nm wavelength

also gradually increases. This reaction design, together with the home-made apparatus, provides an easy characterization way by using UV-Vis spectrophotometer to evaluate the enzyme activity after surface immobilization.

In order to confirm the AChE was immobilized tightly onto the patterned SiO_2/Si substrate, we withdrew the reaction mixture from catalytic surface to a cuvette when reaction had proceeded 2 min and then incubated in a cuvette for more 2 min, in this period, two times of detection followed at accumulation time 8 min and 20 min respectively. No increment of TNB concentration was found, that was no TNB produced if the reaction mixture was removed from catalytic surface. Reload the previous reaction mixture to catalytic surface at accumulation time 10 min; the reaction immediately started again. At accumulation time 18 min, we withdrew the reaction mixture, and the reaction terminated again, shown as figure 13.

3-3 Estimate amount of immobilized AChE on surface silicon wafer

According to coordinate vector of generalized unit cell (Figure 14), a unit cell is defined by six numbers: the lengths of three unique edges, **a, b** and **c**; and five unique angles, **α, β, γ, ψ** and **ρ**. Thus, the volume of crystal is obtained by

$$V = \vec{X} \times \vec{Z} \bullet \vec{Y} = \left| \begin{vmatrix} \hat{i} & \hat{j} & \hat{k} \\ a & 0 & 0 \\ c\cos\beta & 0 & c\sin\beta \end{vmatrix} \bullet (b\cos\gamma, b\cos\rho, b\cos\psi) \right|$$

$$= \left| (0, -ac\sin\beta, 0) \bullet (b\cos\gamma, b\cos\rho, b\cos\psi) \right|$$

$$= \left| -abc\cos\rho\sin\beta \right| = abc\cos\rho\sin\beta \cdots\cdots\cdots(1)$$

Setting coordinate vector of "b" point as:

$$b = \sqrt{b^2\cos^2\gamma + b^2\cos^2\rho + b^2\cos^2\psi}$$

$$\Rightarrow \cos^2\gamma + \cos^2\rho + \cos^2\psi = 1 \cdots\cdots\cdots\cdots(2)$$

By projecting the vector of the point c onto the coordinate vector of the point b and we get

$$c\cos\alpha = c\cos\beta\cos\gamma + 0 + c\sin\beta\cos\psi$$

$$\Rightarrow \cos\psi = \frac{\cos\alpha - \cos\beta\cos\gamma}{\sin\beta} \cdots\cdots\cdots\cdots(3)$$

To substitute eq (3) into eq (2); we get

$$\cos\rho = \sqrt{(1 - \cos^2\gamma - \frac{\cos^2\alpha + \cos^2\beta\cos^2\gamma - 2\cos\alpha\cos\beta\cos\gamma}{\sin^2\beta})} \cdots\cdots\cdots(4)$$

Substituting eq(3) into eq(1), we get the volume of crystal:

$$V = abc\sqrt{\left(\sin^2\beta - \cos^2\gamma\sin^2\beta - \cos^2\alpha - \cos^2\beta\cos^2\gamma - 2\cos\alpha\cos\beta\cos\gamma\right)}$$
$$= abc(1-\cos^2\alpha-\cos^2\beta-\cos^2\gamma+\cos^2\gamma\cos^2\beta$$
$$-\cos^2\gamma\cos^2\beta+2\cos\alpha\cos\beta\cos\gamma)^{1/2}$$
$$= abc(1-\cos^2\alpha-\cos^2\beta-\cos^2\gamma+2\cos\alpha\cos\beta\cos\gamma)^{1/2}\cdots\cdots\cdots(5)$$

According to the Protein Data Base, the unit cell of crystallized *acetylcholinesterase*, *AChE* (ID:1EEA), has the following parameters: a = 140.86 Å, b = 201.46 Å, c = 235.77 Å; α = 90.00°, β = 90.00°, γ = 90.00° ; the molecular weight of the unit AChE: 60 KDa . We can roughly estimate the mean diameter D of the unit AChE (D_{AChE}) as:

$$\frac{\pi}{6}D^3 \le (Volume) = abc\,(1-\cos^2\alpha-\cos^2\beta-\cos^2\gamma+2\cos\alpha\cos\beta\cos\gamma)^{1/2}$$

Thus, we obtained:

$$D_{AChE} \le \left[\frac{6}{\pi}(Volume)\right]^{1/3} = \left[\frac{6}{\pi}\left(abc\,(1-\cos^2\alpha-\cos^2\beta-\cos^2\gamma+2\cos\alpha\cos\beta\cos\gamma)^{1/2}\right)\right]^{1/3}$$

Substituting the parameters into the above equation, we get:

$D_{AChE} \le 233.78$ Å $= 2.3378*10^{-8}$ m ; r $\le 1.1689*10^{-8}$ m $= 1.1689*10^{-7}$ dm.

We calculate the area of the microfludic channel and get 0.1408 dm^2.

As mentioned above, we find out the mean diameter D of the unit AChE (r_{AChE}) and get the area of the unit AChE:

$\pi r^2 = 4.292*10^{-14}$ dm^2/unit.

We assume that the unit AChE was immobilized on one plane on the surface. Thus, we can roughly estimate the amount of AChE immobilized on the surface of a silicon wafer.

$$\frac{0.1408\ dm^2}{4.292*10^{-14} dm^2/unit} = 3.28*10^{12} unit\ (AChE)$$

$$3.28*10^{12}\ unit \times \frac{1\ mole}{6.02*10^{23}\ unit} = 5.466*10^{-12}\ mole$$

$$\frac{X\ (g)}{60*10^3\ Da} = 5.466*10^{-12}\ mole \Rightarrow X = 3.27*10^{-4}\ mg$$

We estimate that the amount of immobilized AChE is $3.27*10^{-4}$ mg on the surface of a silicon wafer in the region of the microfludic channel. Consequently, we can convert the unit (V^*_{max}/H (μM/min)) kinetics of immobilized enzyme into the unit (V_{max} (μmole/min/mg))

3-4 Kinetics assay of soluble AChE

For determining soluble AChE activity, we firtst need to know appopriate enzyme concentration. So we have measured appropriate enzyme activity by fixed saturating substrate concentration and added in various eznyem concentration [39, 40]. As the following steps, we analyzed datas that could find its linear range from 0.5 to 4.5 nM as shown in Figure 15. So that we selected this linear range for our standard assay in all of soluble AChE activity.

Owing to studying enzyme kinetics of AChE, we detected product of 2-nitro-5-thiobenzoic acid (TNB). The complete assay mixture contained the following components: 4 mM to 0.015 mM ATChI, 0.1 mM DTNB, 10 mM potassium phosphate buffer (pH8.0) and effective range of AChE concentration in a final volume of 1000 λ. In the enzymatic kinetics experiment, figure 16 shows kinetic parameters for the soluble AChE, K_m and V_{max}. It were assayed at substrate concentration from 0.015 to 4 mM ATChI and 0.1 mM DTNB added in 10 mM PB buffer (pH 8). According to the Michaelis–Menten equation, the K_m of soluble AChE was 0.791 ± 0.008 mM and the V_{max} was 158.875±5.504 μmole/min/mg.

3-5 Enzymatic activity of surface-immobilized AChE based on running controls

The typical time course plots of product yield are presented in Figure 17 were the TNB absorbance responses to high/low feed concentration of substrate with a series of space times τ (min), after subtracting blank controls with automatic program. It should be emphasized that assay were set up by the scheme (Figure 6) and obtain respective running blank controls: (1) free substrate ATChI for AChE assay, (2) enzyme free, by use of bypass scheme to skip reaction solution directly to UV-Vis spectrophotometer, for AChE assay. Because the values of TNB absorbance at high concentration of substrate ATChI were significantly different from those at low

concentration of substrate ATChI, bypass was an essential strategy to continuous-flow assay of surface-immobilized AChE in order to subtract accurate blank controls.

3-6 Immobilized AChE kinetics: Utilizing automatic program for iterating scheme to determine V^*_{max}/H, corresponding deactivation curve, and K^*_m

As mentioned above, we have already developed the theoretical model for automatic program according to scheme of theoretical model. Thus, we could obtain the kinetic parameters, easily. The determination of V^*_{max}/H for immobilized AChE can be achieved easily using three parts of automatic program under saturating substrate condition, which was 1000 μM substrate ATChI. Due to solubility limit of substrate ATChI in immobilized AChE assay, the initial approximations of V^*_{max}/H (Figure 18) and corresponding deactivation curve (r = 0 in Figure 19(a) were obtained from eq (2) using 1000 μM ATChI as inlet condition of high substrate concentration. This decay curve (r = 0) and 50 μM ATChI as inlet condition of low substrate concentration were then used to obtain the initial approximation of K^*_m (r = 0 in Figure 19 (b)) from eq (1.2). Substituting $< V^*_{max}/H >_o$ and $< K^*_m >_o$ as the initial estimations into the set of two iterating eqs (1.3) and (1.4), the converged results of immobilized AChE were got, through five successive approximations as Figures 19 (a) and 19 (b), as follows: the deactivation curve $\frac{V^*_{max}}{H} = 10.31 + 24.86e^{-0.01292t}$

with R^2 = 0.958, original V^*_{max}/H = 25.95 μM/min, and average K^*_m = 45.66 μM (Figure 20). Because the substrate concentration enough high, but not saturating was satisfied well, the kinetic parameters could be correctly obtained through this iterating calculation (Figure 7). In table 2, comparing immobilized AChE K^*_m (45.66 μM) with homogeneous AChE K^*_m (79.10 μM) implied that there was almost no influence on the affinity of substrate ATChI with immobilized AChE. But an decrease V_{max} (μmole/min/mg) in once an enzyme has been immobilized, indicates that the immobilized enzymes have an apparent lower catalytic rate than that of the free enzyme does, which may be caused by the change of the conformation. There are several reasons why a different kinetic behavior is observed with an enzyme immobilized into a solid support relative to the free enzyme. Firstly, the immobilization may cause some conformational changes in the enzyme molecules. Secondly, the immobilized enzyme is located in an environment different from that when it is the free solution, and this can have a significant effect on the kinetics. Finally, being a membrane enzyme, AChE would not be at the natural optimal conformation both in free-state in solution and immobilized-state on supporting material.

IV Conclusions

Nowadays, enzyme immobilization becomes an necessary for biosensing, bio-regulation and many other bioengineering applications. Because advantage of limited enzyme includes: surmount the stability, recovery, recyclability disadvantages of using enzymes in solution, making them industrially and commercially viable. There are many method for enzyme immobilization, such as adsorption that involves physical surface interactions between the support matrix and the enzyme and can be driven by combined hydrogen bonding, electrostatic forces, and hydrophobic effects; Covalent attachment involves binding amino acid residues (NH_2, CO_2, SH) of the enzyme to the support matrix. This method is popular for high surface area support matrixes with large pore diameters where substrate and product can freely diffuse without the worry of enzyme leaching. Owing to AChE is not free in solution but a membrane anchored protein in the organism, we selecte covalent attachment to immobilize AChE on planar silicon oxide surface in order to simulating AChE anchored on cell membrane like in *vivo*.

Following previously kinetic model for the determination of the kinetics of the immobilized enzyme, we successfully measured the kinetics of the immobilized enzyme. Besides, well-known procedures are available for the kinetic analysis of homogenous enzymes in solution. Besides, we estimated that the amount of

immobilized AChE on the surface of a silicon wafer in the region of the microfludic channel in order to converting the kinetic unit of immobilized enzyme. Then, we could compare the enzymatic kinetics of immobilized and free enzyme in the same kinetic unit. Finally, we compared immobilized AChE K^*_m (45.66 μM) with homogeneous AChE K^*_m (79.10 μM) implied that there was almost no influence on the affinity of substrate ATChI with immobilized AChE. But an decrease V_{max} (μmole/min/mg) in once an enzyme has been immobilized, indicates that the immobilized enzymes have an apparent lower catalytic rate than that of the free enzyme does, which may be caused by the change of the conformation. Besides, according to process of model, we further developed the automatic program for analysis kinetic parameters of immobilized enzyme in order to getting the kinetic parameters of immobilized enzyme as soon as possible by operating the analysis program.

Based on our previously proposed model, we constructed systematic and standard system for analysis of kinetics of immobilized enzymes. Using this prototype platform, it allowed us to observe the kinetic in-situ change of immobilized enzyme, and the advanced fundamental research about kinetic mechanism under different stress conditions could be possible.

V Appendix

I. Theoretical model of micro-fluidic reactor system

According to the model which have been published by our lab [32] that we have constructed a novel home-made micro-fluidic system (Figure 6) for assay enzymatic kinetics parameter of immobilized enzyme. This novel model combined plug flow approximation, Michaelis-Menten equation, and surface reaction limited condition, to fit the kinetics of immobilized enzyme on one-side planar surface as eq (1).

$$\tau = \frac{-K_m^*}{V_{\max}^* / H} Ln(1-\alpha_\tau) + \frac{[S]_o}{V_{\max}^* / H} \alpha_\tau \qquad (1)$$

where space time (τ) is the time required to process the volume of reaction mixture in reactor, K^*_m is the Michaelis constant (mol dm^{-3}) for immobilized enzymes on the planar surface, V^*_{max} is maximum reaction rate per unit surface area of catalyst (mol dm^{-2} min^{-1}), H is the height of rectangular channel reactor, α_τ is reaction conversion fraction, and $[S]_o$ is the substrate concentration at inlet of the channel. Surface reaction limited condition means that diffusion is fast compared to surface reaction. To meet this requirement, the ratio of the reaction volume to the catalytic planar surface must be reduced. We built a micro-fluidic bioreactor with a much smaller channel height than the diffusion layer in semi-infinite diffusion process, and the corresponding dynamic model was discussed in detail in our past reference [32]. By using a series of variant flow rates (or space times), this equation could allow us to

precisely predict the kinetics of immobilized enzyme at different inlet concentration of substrate; details are as followings:

If reaction conversion fraction, α_τ, is smaller than 1%, and $[S]_o$ is much higher than K^*_m, then eq (1) can be degenerated as follows:

$$\alpha_\tau \approx < \frac{V^*_{\max}}{H} >_0 \left(\frac{\tau}{[S]_{o,H}}\right) \qquad (for\ [S]_{o,H} >> K^*_m) \qquad (2)$$

where the subscript H of $[S]_{o,H}$ refers to this saturating assay condition, the subscript 0 of $< \frac{V^*_{\max}}{H} >_0$ refers to initial approximation without regard to K^*_m factor. This condition means that the highest available concentration of substrate is much larger than K_m. If we could choose $[S]_{o,H} \geq 19K_m$, then the error involved in the approximation of $< \frac{V^*_{\max}}{H} >_0$ based on eq (2) would be less than 5%. Eq (2) provides us to determine $< \frac{V^*_{\max}}{H} >_0$ using linear regression, and the discrete determined values of $< \frac{V^*_{\max}}{H} >_0$ could be used to fit a decay curve concerning the issue of deactivation of immobilized enzyme; therefore the any simultaneous value of $< \frac{V^*_{\max}}{H} >_0$ can be determined in experiment progress. Eq (1) obviously indicates that we should choose as low as possible the $[S]_o$ concentration, as long as the output concentration of reporter is not beyond the limit of detection, to increase the accuracy of K^*_m evaluation after $\frac{V^*_{\max}}{H}$ determined as above. Eq (1) can be arranged into the following eq:

$$< \frac{V_{\max}^*}{H} >_0 \tau - [S]_{o,L}\alpha_\tau = - < K_m^* >_0 Ln(1-\alpha_\tau) \qquad (1.2)$$

where the subscript L of $[S]_{o,L}$ refers to at low concentration of substrate, the subscript 0 of $< K_m^* >_0$ refers to an initial approximation. With linear regression of eq (1.2), and using a set of space time τs and the corresponding measured data of conversion fraction α_τs, we can derive estimated value for $< K_m^* >_0$, the slope of eq (1.2). If the $[S]_{o,H}$ can be prepared to guarantee the saturating assay condition, then $< \frac{V_{\max}^*}{H} >_0$ and $< K_m^* >_0$ determined by eq (2) and eq (1.2) respectively, will be good approximations.

Nevertheless, the saturating substrate condition can't always be achieved in some assays because of high-substrate inhibition or limit of substrate solubility. If the highest available concentration of substrate is larger than the level of $3K_m$, then accurate estimates of kinetics for immobilized enzymes can still be achieved. For this case, considering an iterative scheme, we can re-arrange eq (1) as eq (1.3), and combine eq (1.3) with eq (1.2) to set up the following set of equations.

$$\begin{cases} < \frac{V_{\max}^*}{H} >_r = \frac{1}{\tau}\{- < K_m^* >_{r-1} Ln(1-\alpha_\tau) + [S]_{o,H}\alpha_\tau\} & (1.3) \\ < \frac{V_{\max}^*}{H} >_r \tau - [S]_{o,L}\alpha_\tau = - < K_m^* >_r Ln(1-\alpha_\tau) & (1.4) \end{cases}$$

Where r = 1, 2, 3, …, and $< K_m^* >_0$ obtained by eq (1.2) as the initial approximation for eq (18.3). For optimum estimations of $\frac{V_{\max}^*}{H}$ and K_m^*, the detected values of in eq (1.3) and eq (1.4) are based on two measurement conditions – high inlet

concentration of substrate, $[S]_{o,H}$, and low inlet concentration of substrate, $[S]_{o,L}$, respectively. After successively finite computing, we will get repetitions of decimal places being used for $< \frac{V^*_{\max}}{H} >_r$ and $< K^*_m >_r$, and these values are then the final approximate solutions to eq (1.3) and eq (1.4), respectively.

As mentioned above, this method will fail or gain a large deviation from true value of kinetics when the highest available concentration of substrate is far lower than saturation (i.e., $\leq 3K_m$). This is similar to the limitations of Michaelis-Menten plot to estimate the kinetic value of homogeneous catalytic reaction. The strategy of measurement and calculation is briefly outlined as Figure 7.

References

1. Thies, W., Bleiler, L. (2011) Alzheimer's disease facts and figures. *Alzheimers Dement*. **7**: 208-44.
2. Rosenberry, T.L. (1975) *Acetylcholinesterase*. *Adv Enzymol Relat Areas Mol Biol*. **43**: 103-218.
3. Mather, J.A. (2005) Alzheimer's disease. *Choice: Current Reviews for Academic Libraries*. **43**: 323-324.
4. Smith, C. (2009) Alzheimer's Disease: Facing the facts. booklist. **105**: 89.
5. Eberhart, G.M. (2003) Encyclopedia of Alzheimer's Disease. *College & Research Libraries News*. **64**: 277.
6. Otte, R.L. (2001) Alzheimer's disease/heart disease (Book Review). Book Report. **19**: 71.
7. Johnson, C. (2007) Focus: Alzheimer's disease resources. *Medicine on the Net.* **13**: 18-18.
8. Martin, R.E. (2010) Plain Talk about Alzheimer's disease: Alzheimer's related dementia and wandering. *Christian Librarian*. **53**: 83-83.
9. Starkstein, Sergio E., Dragovic, Milan., Jorge, Ricardo., Brockman, Simone ., Robinson., Robert, G., (2011) Diagnostic criteria for depression in Alzheimer disease: a study of symptom patterns using latent class analysis. *Am J Geriatr Psychiatry.* **19**: 551-8.
10. Patricia, A. Wilkosz., Chowdari, Kodavali., Elise, A. Weamer., Sachiko Miyahara., Oscar, L. Lopez., Vishwajit, L. Nimgaonkar, Steven, T. DeKosky., Robert, A. Sweet., (2007) Prediction of psychosis onset in Alzheimer disease: the role of depression symptom severity and the HTR2A T102C polymorphism. *Am J Med Genet B Neuropsychiatr Genet.* **144B**: 1054-62.

11. Tschanz, J.T., Corcoran, C.D., Schwartz, S., Treiber, K., Green, R.C., Norton, M.C., Mielke, M.M., Piercy, K., Steinberg, M., Rabins, P.V., Leoutsakos, J.M., Welsh-Bohmer, K.A., Breitner, J.C., Lyketsos, C.G. (2011) Progression of cognitive, functional, and neuropsychiatric symptom domains in a population cohort with Alzheimer dementia: the Cache County Dementia Progression study. *Am J Geriatr Psychiatry.* **19**: 532-42.

12. Terry, R.D. (2000) Cell death or synaptic loss in Alzheimer disease. *J Neuropathol Exp Neurol.* **59**: 1118-9.

13. Egan, T. (1990) As memory and music faded, Alzheimer patient met death.

14. Stern, Y., Tang, M.X., Albert, M.S., Brandt, J., Jacobs, D.M., Bell, K., Marder, K., Sano M., Devanand D., Albert S.M., Bylsma F., Tsai W.Y. (1997) Predicting time to nursing home care and death in individuals with Alzheimer disease. *JAMA.* **277**: 806-12.

15. Pappolla, M.A., Sos, M., Omar, R.A., Bick, R.J., Hickson-Bick, D.L., Reiter, R.J., Efthimiopoulos, S., Robakis, N.K. (1997) Melatonin prevents death of neuroblastoma cells exposed to the Alzheimer amyloid peptide. *J Neurosci.* **17**: 1683-90.

16. Frecker, M.F., W.E.M. PrysePhillips., H.R. Strong. (1995) Alzheimer's disease death certificates. *Neurology*. **45**: 2298-2298.

17. Beard, C.M., Kokmen, E., Sigler, C., Smith, G.E., Petterson, T., O'Brien, P.C. (1996) Cause of death in Alzheimer's disease. *Annals of Epidemiology*. **6**: 195-200.

18. Hoyert, D.L., Rosenberg, H.M. (1997) Alzheimer's disease as a cause of death in the United States. *Public Health Reports*. **112**: 497-505.

19. Yanagisawa, K. (2000) Neuronal death in Alzheimer's disease. *Internal Medicine*. **39**: 328-330.

20. Raina, A.K. (2002) Neuronal survival and death in Alzheimer disease. *Mapping the Progress of Alzheimer's and Parkinson's Disease*. **51**: 49-57.

21. Borroni, B., Grassi, M., Costanzi, C., Bianchi, M., Padovani, A. (2009) Behavioral dimensions and *acetylcholinesterase* inhibitor-related effect in Alzheimer disease over time: a latent trajectory modeling. C*ogn Behav Neuro.***22**: 222-8.

22. Bartolucci, C., Siotto, M., Ghidini, E., Amari, G., Bolzoni, P.T., Racchi, M., Villetti, G., Delcanale, M., Lamba, D. (2006) Structural determinants of Torpedo californica *acetylcholinesterase* inhibition by the novel and orally active carbamate based anti-alzheimer drug ganstigmine . *J.M.C.* **49**: 5051-8.

23. Lane, R.M., M. Kivipelto., N.H. Greig. (2004) *Acetylcholinesterase* and its inhibition in Alzheimer disease. *Clinical Neuropharmacology*. **27**: 141-9.

24. Kuhl, D.E., Minoshima, S., Frey, K.A., Foster, N.L., Kilbourn, M.R., Koeppe, R.A. (2000) Limited donepezil inhibition of *acetylcholinesterase* measured with positron emission tomography in living Alzheimer cerebral cortex. *Annals of Neurology*. **48**: 391-5.

25. Kamal, M.A., Greig, N.H., Alhomida, A.S., Al-Jafari, A.A. (2000) Kinetics of human *acetylcholinesterase* inhibition by the novel experimental Alzheimer therapeutic agent, tolserine. *Biochemical Pharmacology*. **60**: 561-70.

26. Siek, G.C., Katz, L.S., Fishman, E.B., Korosi, T.S., Marquis, J.K. (1990) Molecular forms of *acetylcholinesterase* in subcortical areas of normal and Alzheimer disease brain. *Biol Psychiatry*. **27**: 573-80.

27. Barshan Tashnizi, M., Ahmadian, S., Niknam, K., Torabi, S.F., Ranaei Siadat S.O. (2005) Covalent immobilization of Drosophila *acetylcholinesterase* for biosensor applications. *Biotechnol Appl Biochem*. **52**: 257-64.

28. Du, D., Chen, S., Cai, J., Zhang, A. (2007) Immobilization of *acetylcholinesterase* on gold nanoparticles embedded in sol-gel film for amperometric detection of organophosphorous insecticide. *Biosens Bioelectron.* **23**: 130-4.

29. Tumturk, H., Sahin, F., Demirel, G. (2007) A new method for immobilization of *acetylcholinesterase*. *Bioprocess Biosyst Eng*. **30**: 141-5.

30. Sahin, F., Demirel, G., Tumturk, H. (2005) A novel matrix for the immobilization of *acetylcholinesterase*. *Int J Biol Macromol*. **37**: 148-53

31. Milkani, E., Khaing, A.M., Huang, F., Gibson, D.G., Gridley, S., Garceau, N., Lambert, C.R., McGimpsey, W.G. (2010) Immobilization of *acetylcholinesterase* in lipid membranes deposited on self-assembled monolayers. *Langmuir*. **26**: 18884-92.

32. Lee, C.C., Chiang, H.P., Li, K.L., Ko, F.H., Su, C.Y., Yang, Y.S. (2009) Surface Reaction Limited Model for the Evaluation of Immobilized Enzyme on Planar Surfaces. Anal. Chem. **81**: 2737-2744.

33. Marinov, I., Gabrovska, K., Velichkova, J., Godjevargova, T. (2009) Immobilization of *acetylcholinesterase* on nanostructure polyacrylonitrile membranes. *Int J Biol Macromol*. **44**: 338-45.

34. Cesar, Mateo., Jose, M. Palomo., Gloria, Fernandez-Lorente., Jose, M. Guisan., Roberto, Fernandez-Lafuente. (2007) Improvement of enzyme activity, stability and selectivity via immobilization techniques. *Enzyme and Microbial Technology.* **40**: 1451-1463.

35. Delouise, L.A., Miller, B.L. (2005) Enzyme immobilization in porous silicon: quantitative analysis of the kinetic parameters for glutathione-S-transferases. *Anal Chem*. **77**: 1950-6.

36. Godjevargova, T., Nenkova, R., Dimova, N. (2008) Immobilization of

acetylcholinesterase on new modified acrylonitrile copolymer membranes. *Journal of Molecular Catalysis B: Enzymatic*. **55**: 169-176.

37. Sanllorente-Mendez., Dominguez-Renedo, S.O., Arcos-Martinez, M.J. (2010) Immobilization of *acetylcholinesterase* on screen-printed electrodes. *Application to the determination of arsenic(III)*. **10**: 2119-28.

38. Fatranská, M., Kiss, A., Oprsalová, Z., Kvetnanský, R. (1989) *Acetylcholinesterase* and choline acetyltransferase activity in some hypothalamic nuclei under immobilization stress in rats. *Endocrinol Exp*. **23**: 3-10.

39. Barr, R.D., Koekebakker, M., Lawson, A.A. (1998) *Acetylcholinesterase* in the human erythron. II. Biochemical assay. *Am J Hematol*. **28**: 260-5.

40. Kiely, J.S., Moos, W.H., Pavia, M.R., Schwarz, R.D., Woodard, G.L. (1991) A silica gel plate-based qualitative assay for *acetylcholinesterase* activity: a mass method to screen for potential inhibitors. *Anal Biochem*. **196**: 439-42.

Clean wafer

Element	Start BE	Peak BE	End BE	Height Counts	FWHM eV	Area (P) CPS.eV	Area (N)	At. %
Si2p	111.49	107.29	103.81	22287.34	2.1	258162.7	174661.03	41.77
O1s	539.82	535.99	532.45	53755.83	1.65	1028982.39	203425.93	48.65
N1s	407.2	403.32	399.51	4312.55	2.83	3403.8	1076.94	0.26
C1s	294.63	288.33	283.18	15238.35	2.73	69270.85	38952.97	9.32

Immobilization step one: 5% APTES

Element	Start BE	Peak BE	End BE	Height Counts	FWHM eV	Area (P) CPS.eV	Area (N)	At. %
Si2p	110.41	107.07	104.18	7044.57	2.05	77513.45	52441.08	16.52
O1s	541.38	536.69	533.1	17055.03	2.1	404773.58	80030.05	25.21
N1s	409.39	404.37	400.94	12145.95	3.03	99266.97	31411.2	9.89
C1s	295.17	290.09	286.64	31265.18	2.32	273038.54	153565.38	48.38

Immobilization step two: 5% APTES + 25% Glutaraldehyde

Element	Start BE	Peak BE	End BE	Height Counts	FWHM eV	Area (P) CPS.eV	Area (N)	At. %
Si2p	111.47	107.36	104.39	4175.67	1.94	44934.6	30400.89	9.79
O1s	541.3	537.42	532.16	14696.73	2.37	392111.6	77534.49	24.96
N1s	409.91	406.45	402.31	9013.85	2.35	50725.75	16055.17	5.17
C1s	295.3	290.03	286.87	24186.84	1.91	331896.57	186667.85	60.09

Immobilization step three: 5% APTES + 25% Glutaraldehyde + Enzyme

Element	Start BE	Peak BE	End BE	Height Counts	FWHM eV	Area (P) CPS.eV	Area (N)	At. %
Si2p	111.97	107.93	104.89	3835.13	2.12	29459.4	19931.99	6.53
O1s	542.09	537.83	534.08	11674.65	2.58	328855.01	65030.12	21.29
N1s	411.16	405.44	401.2	10688.51	2.56	54143.02	17134.72	5.61
C1s	295.67	290.5	287.41	26880.28	2.35	361542.72	203351.53	66.57

Table 1. The percentage of elemental analysis at different stages of immobilization process. While the every immobilized step increases that the percentage of Si elemental analysis reduce, but the percentage of C elemental analysis raises. Thus, we could confirm that the enzyme immobilized onto surface silicon wafer, successfully.

	Immobilized AChE	Free AChE	Assay condition
Immobilization support	Silicon oxide	none	ATChI
V_{max} (μmole/min/mg)	7.2 ± 0.6	159 ± 5	0.1 mM DTNB
K_m (μM)	46 ± 3	79 ± 8	10 mM PB (pH 8)
K_{cat} (min^{-1})	433 ± 36	44485 ± 1541	

Table 2. Experiment-determined catalytic parameters of turnover numbers (k_{cat}) and Michaelis constants (K_m) for the soluble and planar surface–immobilized AChE systems.

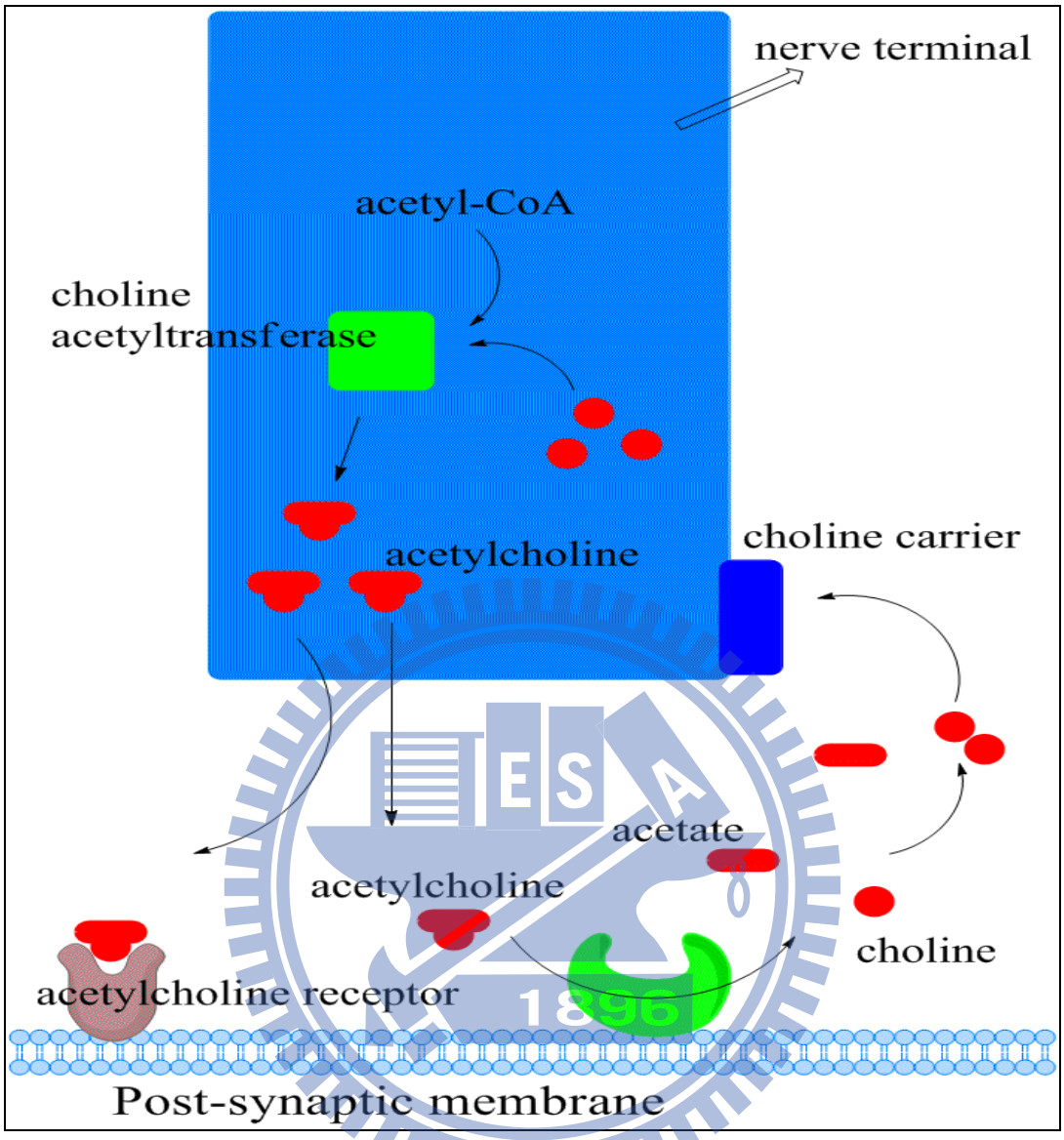

Figure 1. The mechanism of action of acetylcholinesteras (AChE) cholinergic nerve transmission is terminated by the enzyme *acetylcholinesterase* (AChE). AChE is found both on the post-synaptic membrane of cholinergic synapses and in other tissues like red blood cells. Acetylcholine (ACh) binds to AChE and is hydrolysed to acetate and choline. This inactivates the ACh and the nerve impulse is halted. AChE inhibitors prevent the hydrolysis of ACh, which increases the concentration of ACh in the synaptic cleft; AChE inhibitors are widely used in the treatment of Alzheimer's disease.

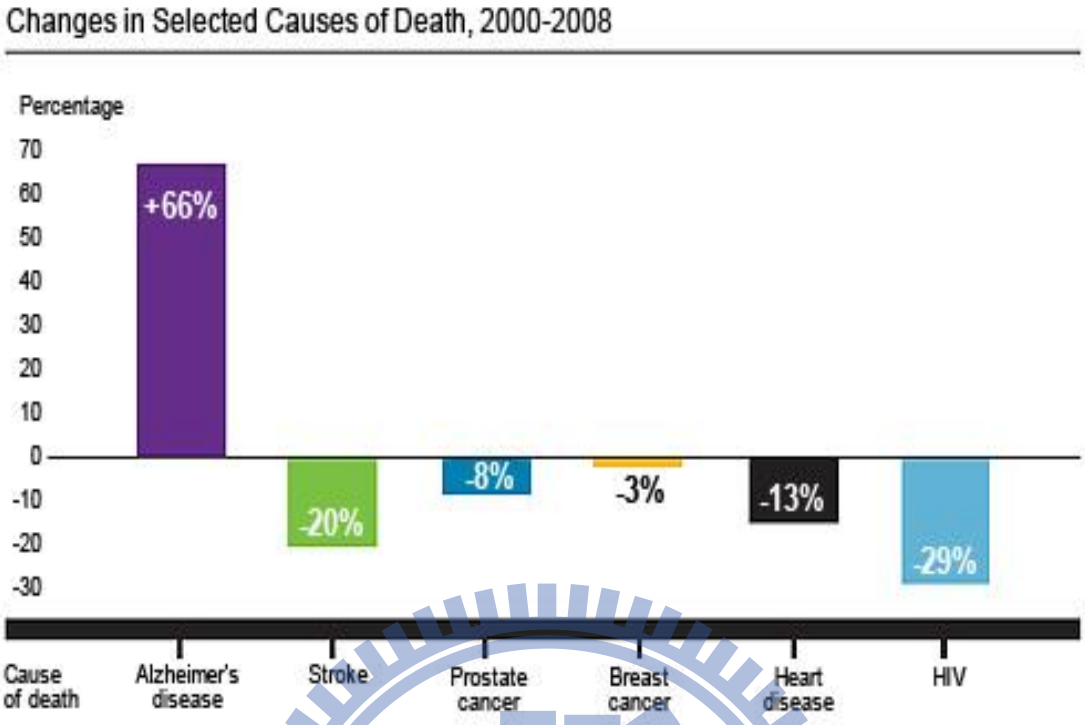

Figure 2. Percentage changes in selected causes of death (all ages) between 2000 and 2008 [1].

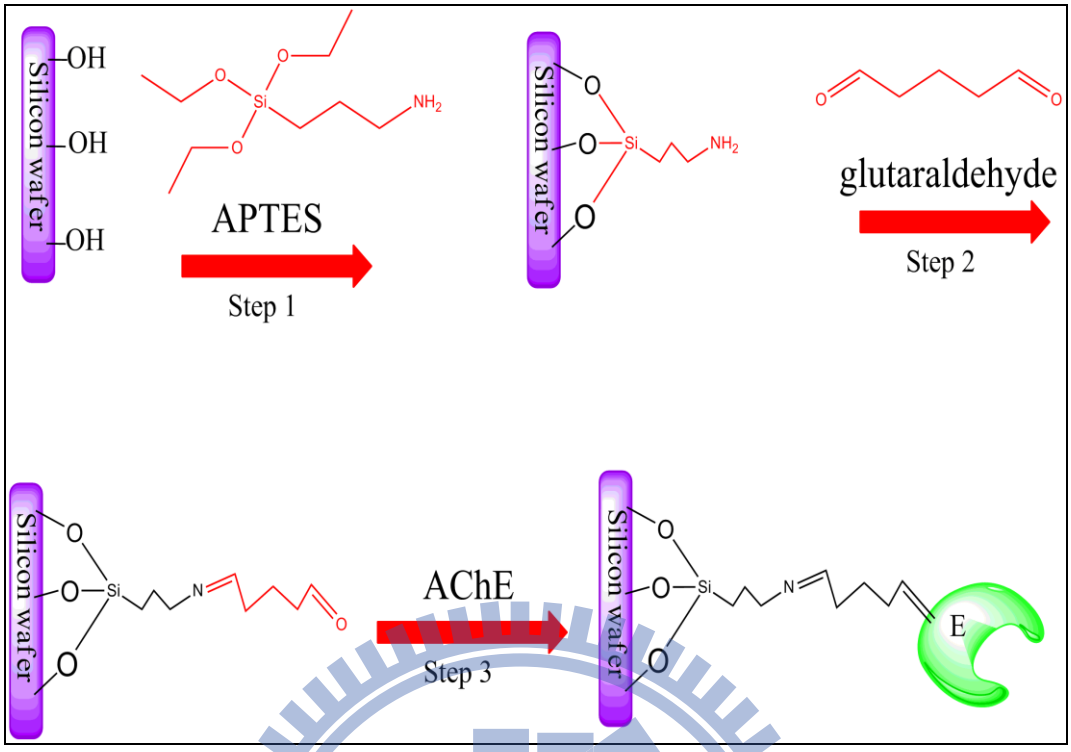

Figure 3. Schematic diagram of the immobilization of AChE onto silicon oxide surface. The immobilized enzyme functionalized on silicon wafer needed three-step reaction of surface modification: We first modified surface of silicon wafer by 3-triethoxysilylpropylamine (APTES) that provided amine groups. At second step, we utilized glutaraldehyde to bind amine groups via covalent binding. At third step, according to Chemical characteristic of aldehyde group is able to bind amine groups of *acetylcholinesterase* (AChE) that would form disulfide bind via covalent binding.

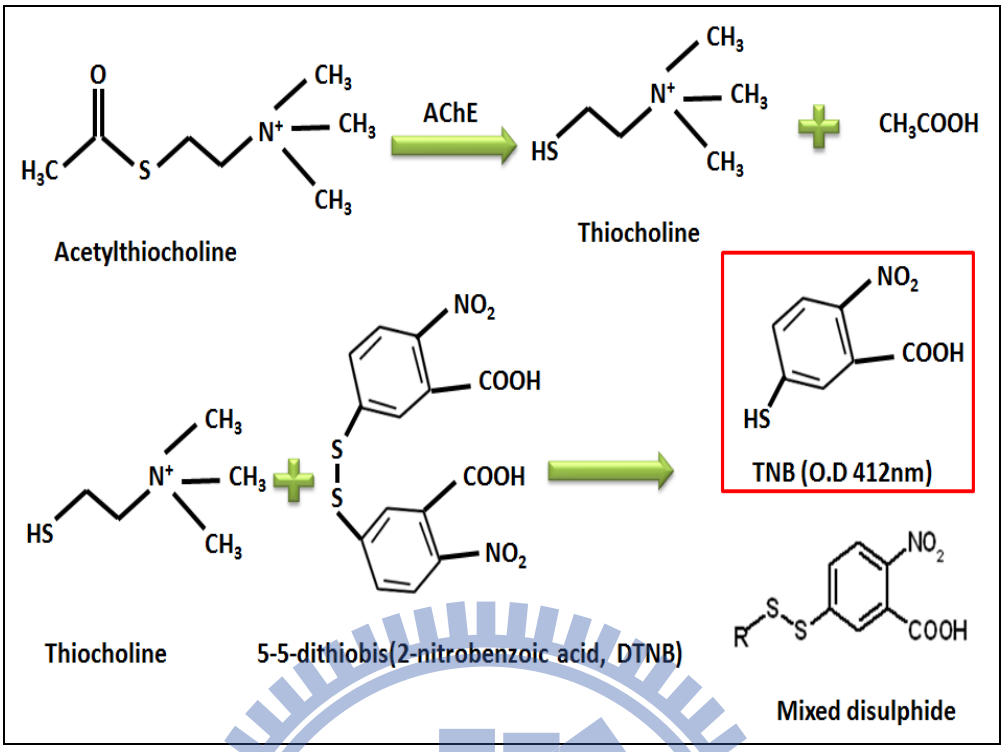

Figure 4. The steps involved in estimation of AChE activity by using Ellman's method. Acetythiocholine (ATChI) is broken down in the presence of *acetylcholinesterase* (AChE) to release thiocholine that reacts with 5,5-dithiobis-(2-nitrobenzoic acid) (DTNB) to rapidly form thionitro benzoic acid (TNB) and detects its absorbance at 410 nm.

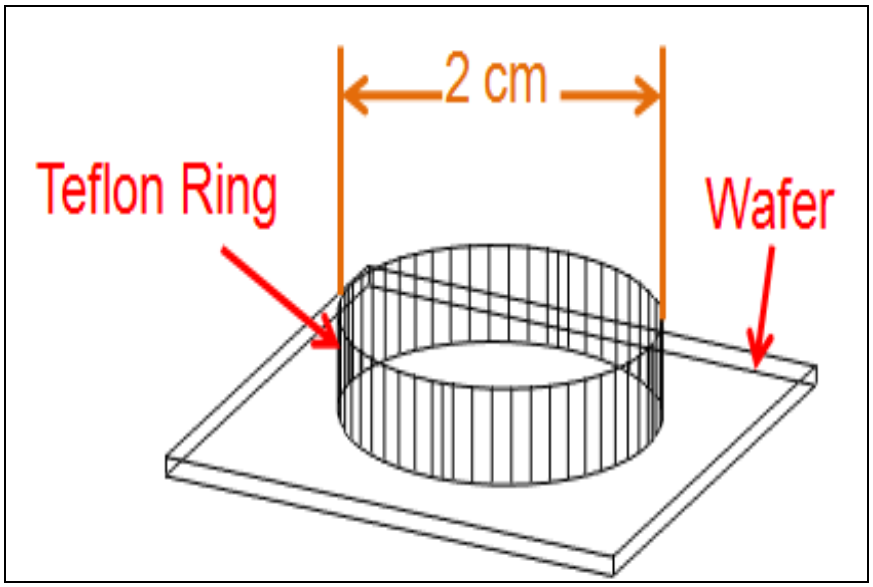

Figure 5. Schematic diagram of the home-made apparatus for immobilization of *acetylcholinesterase* onto the silicon dioxide surface.

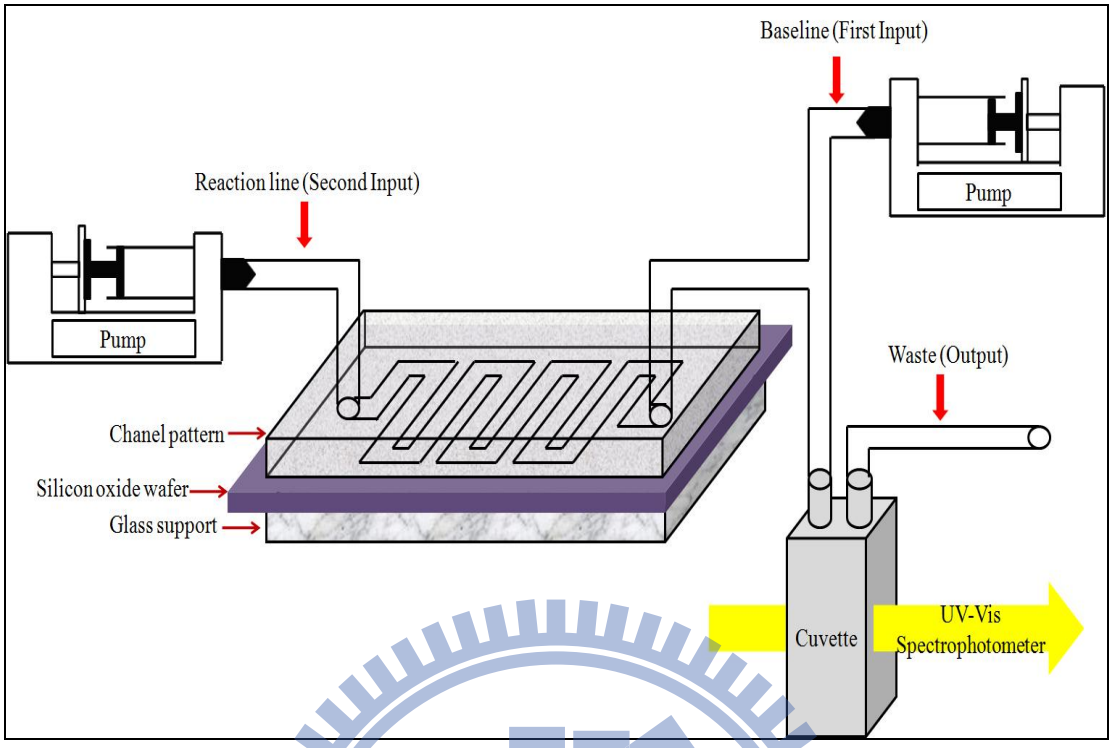

Figure 6. Overview of home–made reactor system for measurement immobilized enzymatic kinetics. Reactor system design for the determination of kinetic constants of immobilized enzyme. Rectangular reactor with a catalytic surface on the silicon oxide wafer. The channel size is $L\,(72.6\,cm)\times W(0.194\,cm)\times H\ (167\,\mu m)$ (where $L >> W >> H$).

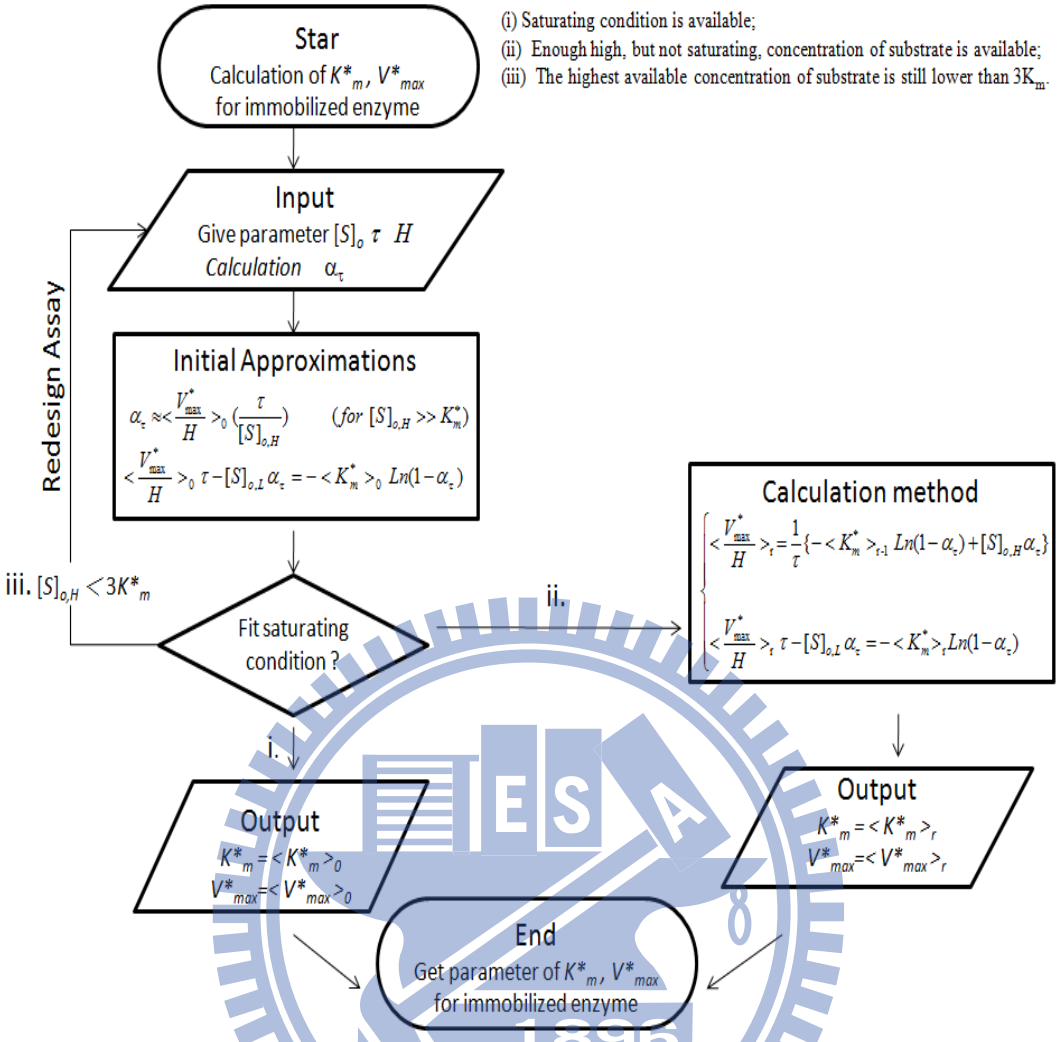

Figure 7. A systematic and standardized data analysis. Flow chart showing the scheme of solving eq (1) to determine the apparent kinetics of immobilized enzyme when i) saturating condition is available; ii) enough high, but not saturating, concentration of substrate is available; iii) the highest available concentration of substrate is still lower than $3K^*_m$. These conditions of choice can be also regarded as the final check for the reasonableness of calculating results.

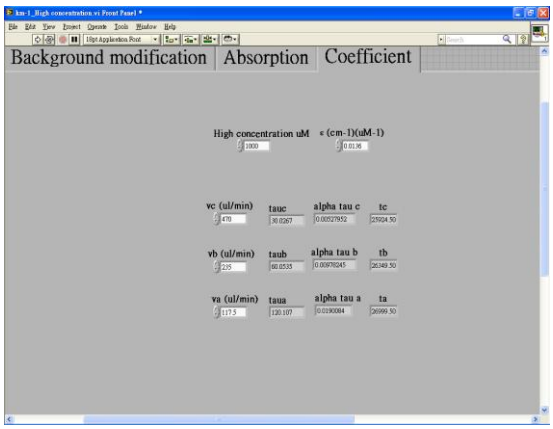

(a)

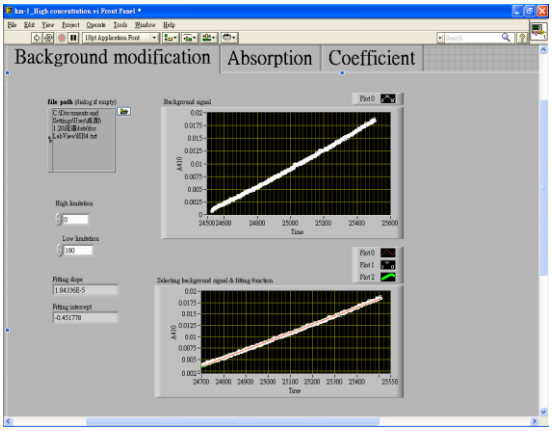

(b)

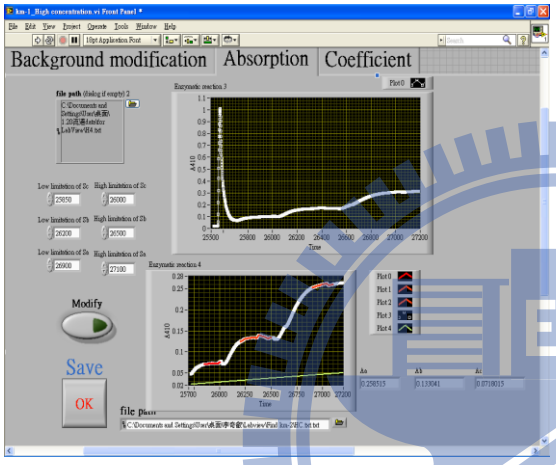

(c)

Figure 8. The first automatic program for modifying progress curves of immobilized-enzyme reaction cycles. (a) To key essential parameters: flow rate (μl/min), space time (min), extinction coefficient of product (ε) and substrate concentration (μM). (b) Entering in the baseline of high/low concentration for background, respectively. (c) To key in reaction line of high concentration and select region for modification and subtract from baseline of high concentration that is operated as same as the low concentration of substrate.

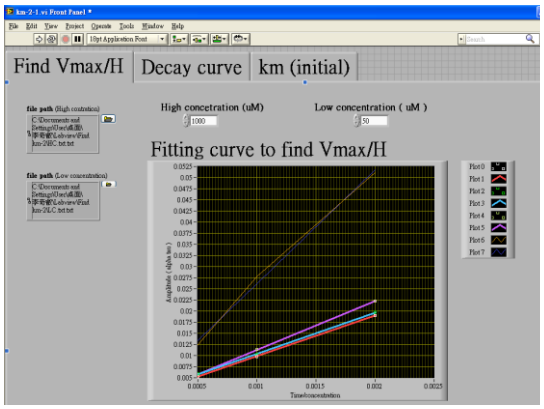

(a)

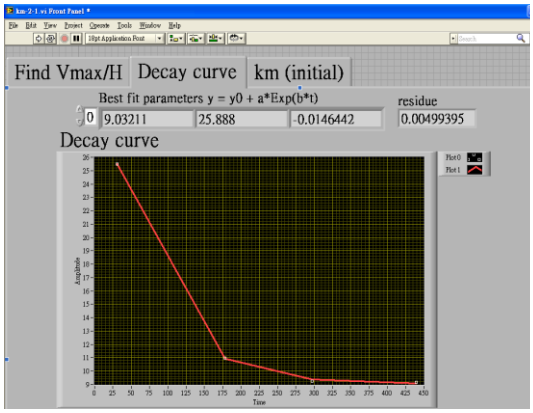

(b)

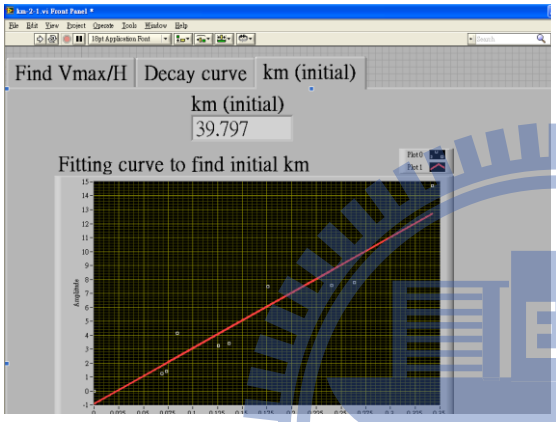

(c)

Figure 9. The second automatic program for computing initial approximation of $<\frac{V_{\max}^*}{H}>_0$, $<K_m^*>_0$ and decay curve about the issue of deactivation of immobilized enzyme. (a)(b) We entered qualified reaction line of high/low concentration and concentration of substrate into program. After computing for first time, we got the initial of $<\frac{V_{\max}^*}{H}>_0$, decay curve of deactivation of immobilized enzyme. (c) According to above parameters, we could figure out the initial $<K_m^*>_0$ of immobilized enzyme.

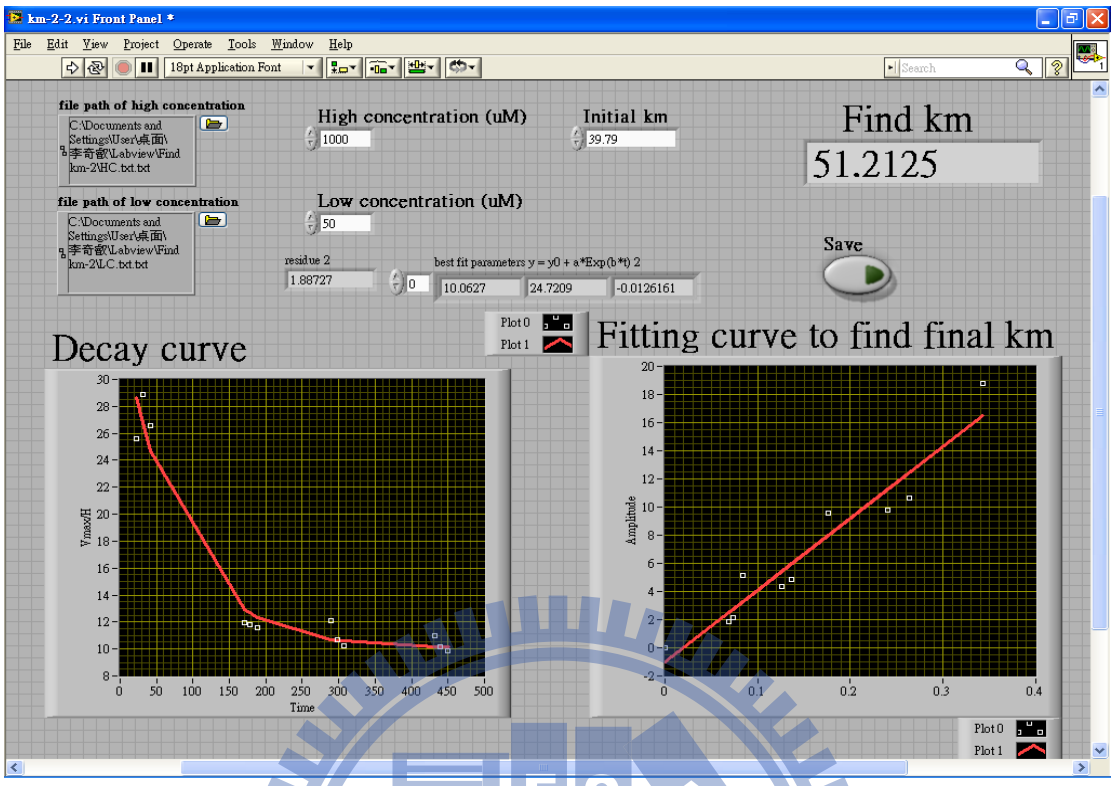

Figure 10. The third automatic program for finding the final value of $< K^*_m >_r$ of immobilized enzyme. The value of final $< K^*_m >_r$ would find out after we entered qualified reaction line of high/low concentration, concentration of substrate and initial $< K^*_m >_0$ into third automatic program.

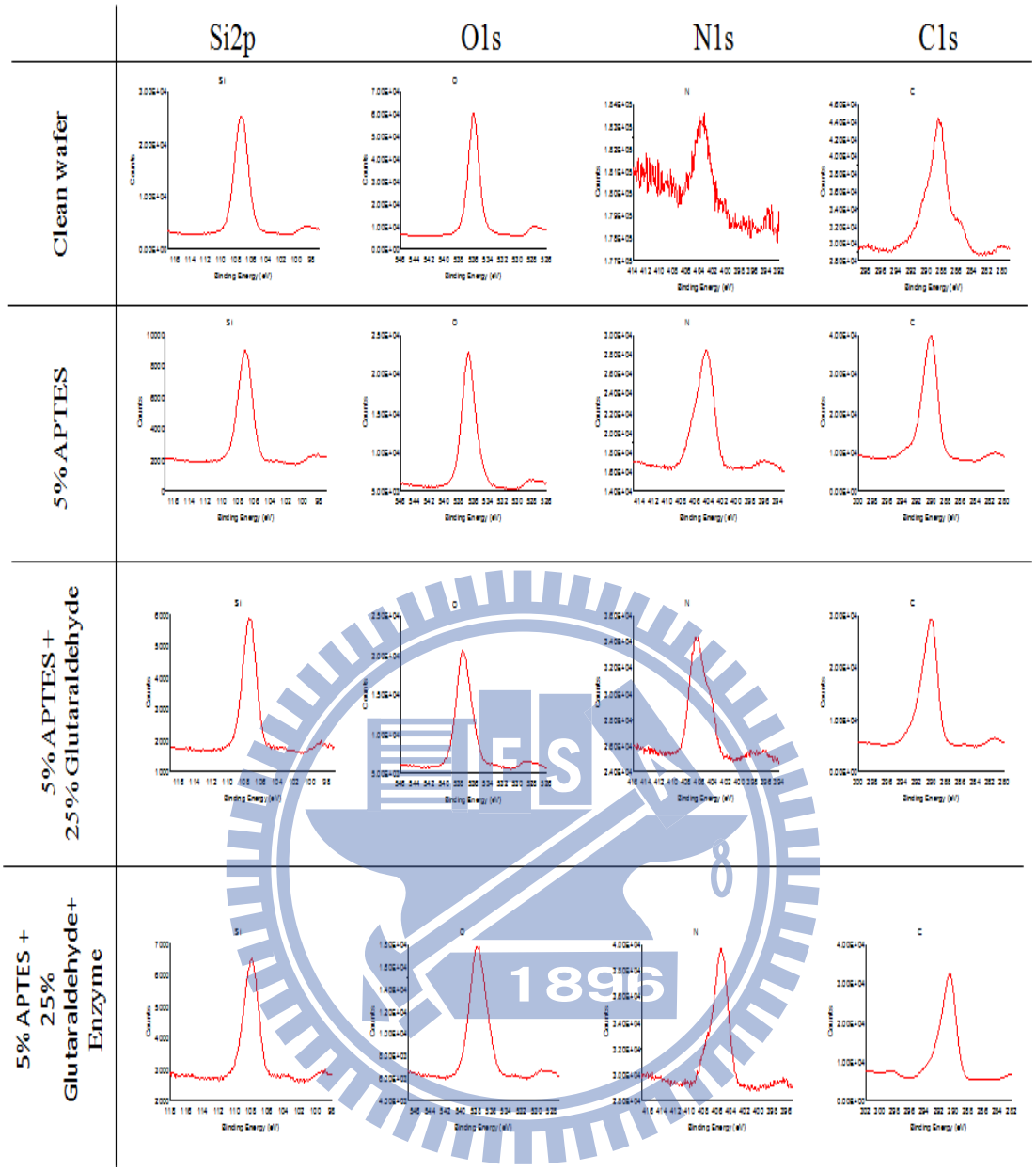

Figure 11. The XPS spectra of each immobilization step. After each immobilization step, we utilized XPS to scan the four element (Si, O, N, C) on surface of silicon wafer.

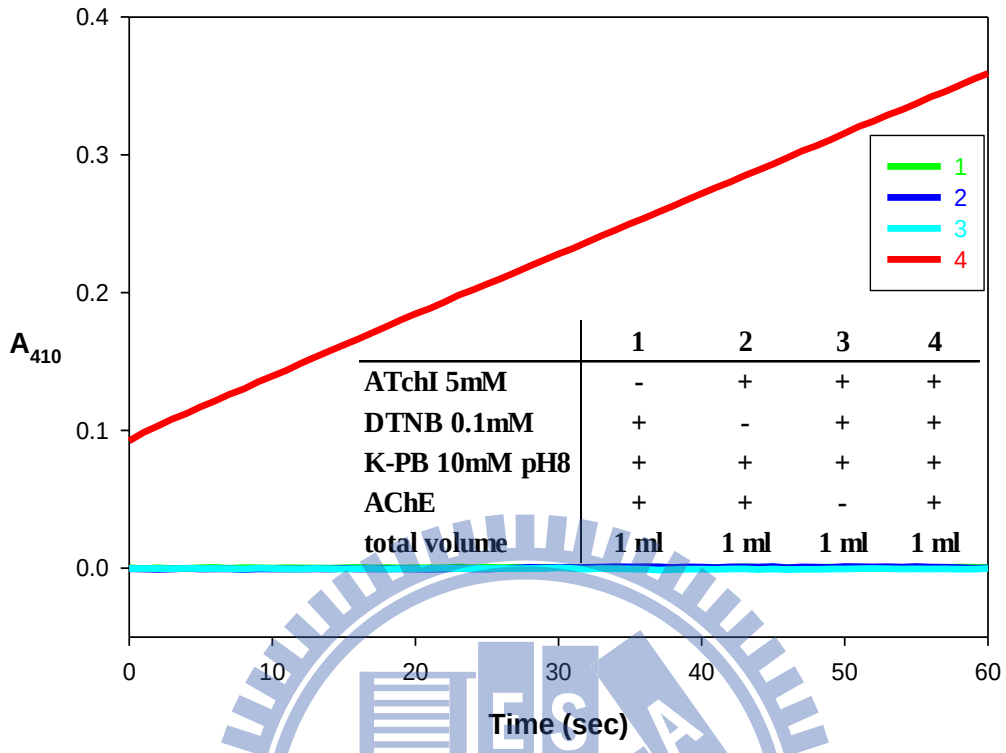

Figure 12. Progress curves of enzyme assay for AChE. Complete reaction. (1) could observe an increase of absorbance at 410 nm but there is no change of absorbance for control reaction without ATChI (2), DTNB (3) and AChE (4). Detailed procedures are described in Materials and Methods.

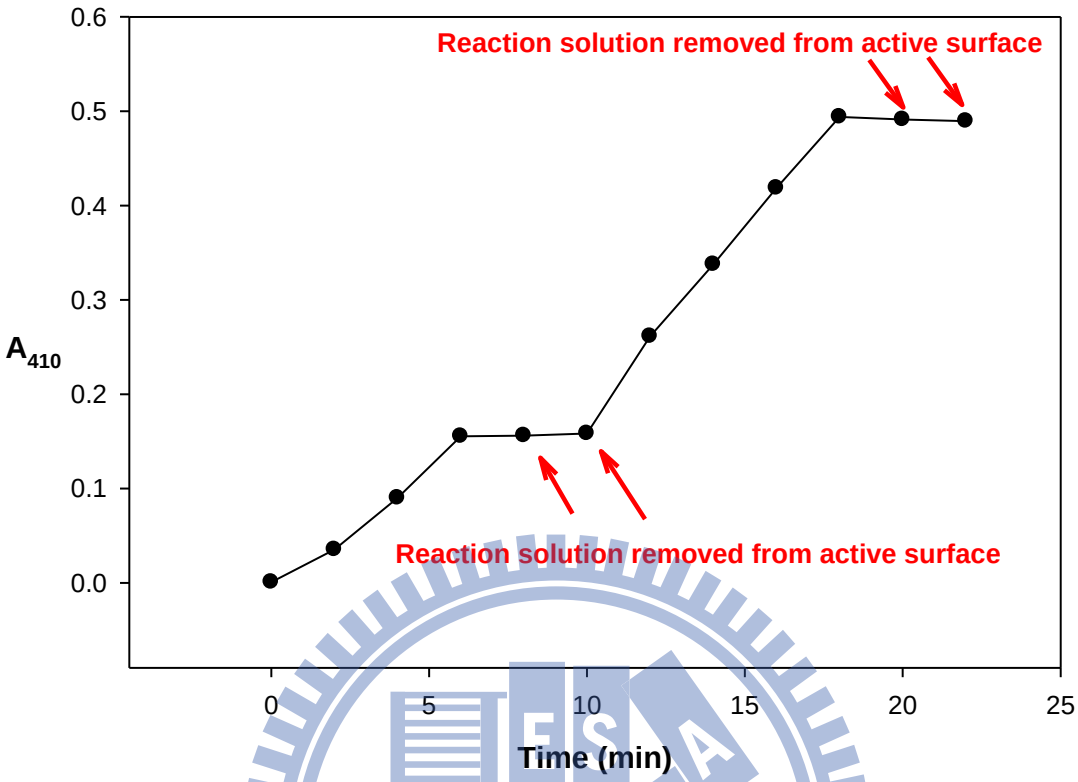

Figure 13. The absorbance of 2-nitro-5-thiobenzoic acid (TNB). Time course with two termination periods caused by removing reaction mixture from catalytic surface and the enzyme target sample (*acetylcholinesterase* immobilized onto the silicon oxide surface).

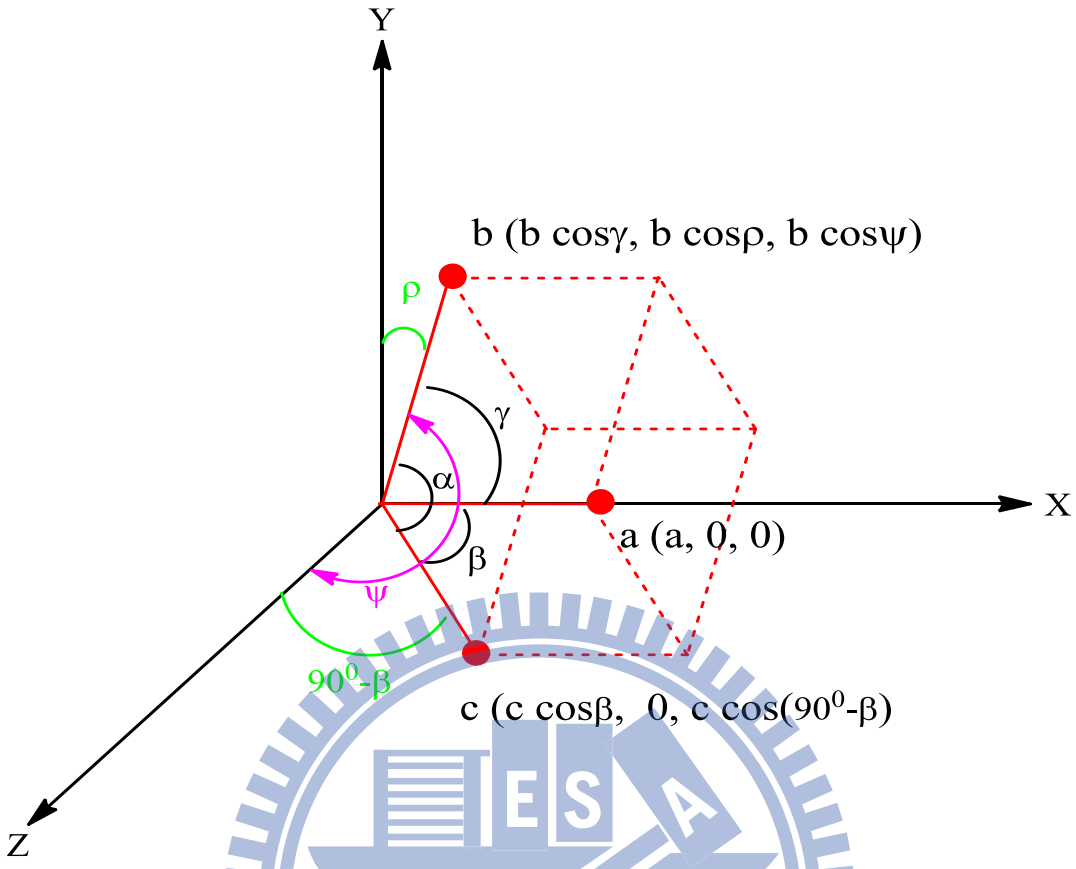

Figure 14. The overview of general crystal with vector coordinate. The crystal of general (triclinic) unit cell, with edges **a, b, c** and angles **α, β, γ, ψ, ρ**.

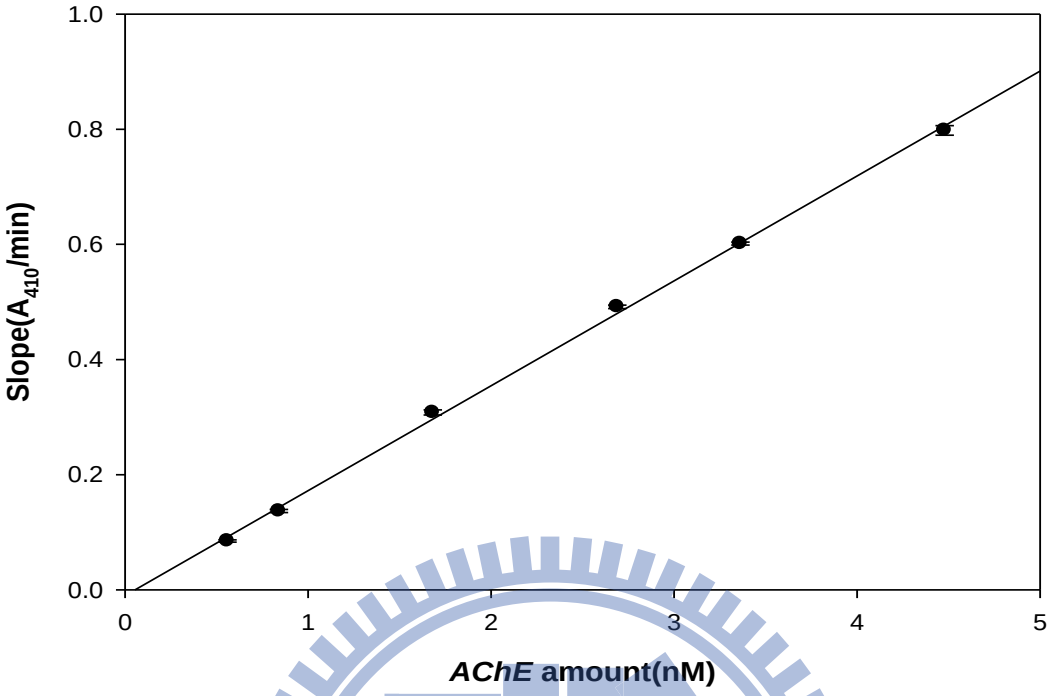

Figure 15. Effective range of AChE assay. AChE catalyzed by the variable amount of AChE (from 0.5 to 4.5 nM) was determined under the standard condition. Each point and bar represented the mean and SD, respectively, obtained from three experiments.

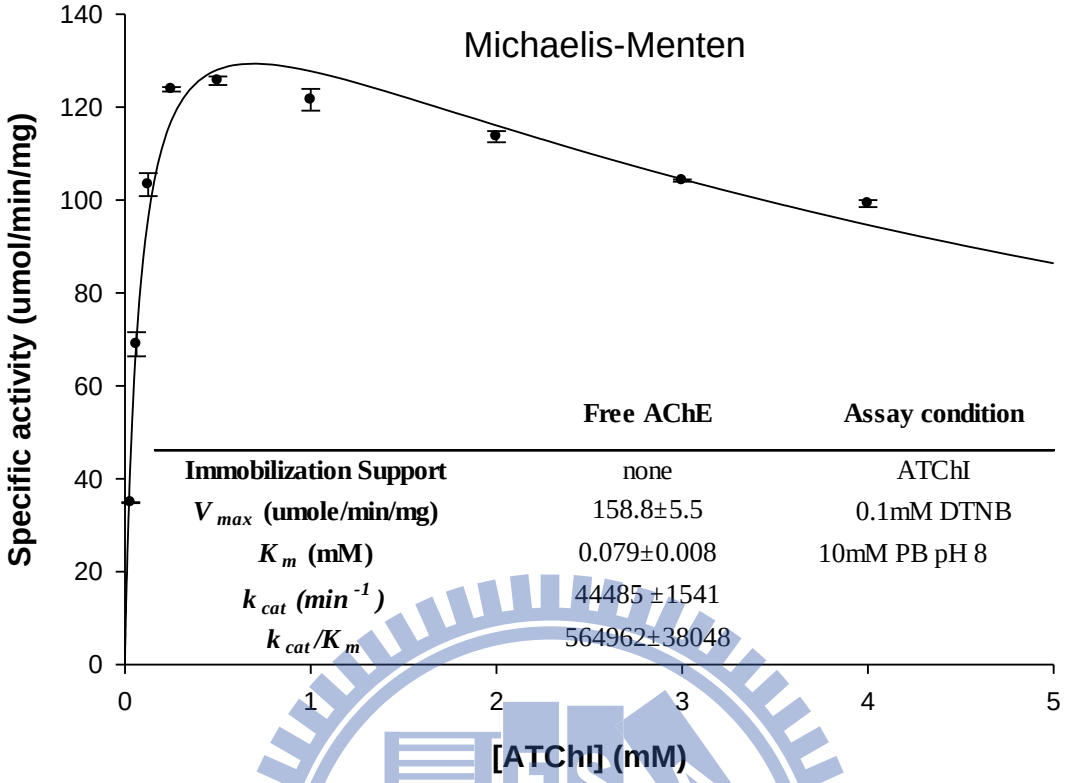

Figure 16. Michaelis-Menten plots for hydrolysis reaction by free AChE. Lines of best fit were obtained from the data using Enzyme Kinetics Module software. Each point and bar represented the mean and SD, respectively, obtained from three experiments.

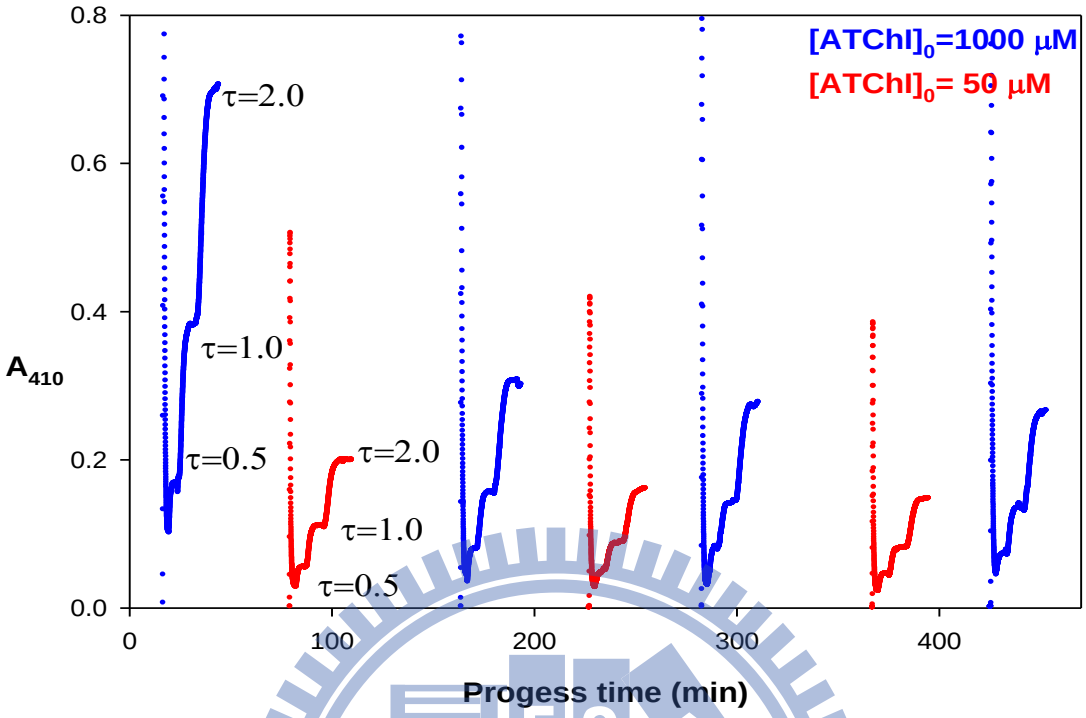

Figure 17. The typical progress curves of enzymatic assays. The absorbance measurements of time courses were obtained after setting zero on a control solution containing no ATChI substrate in the AChE assay.

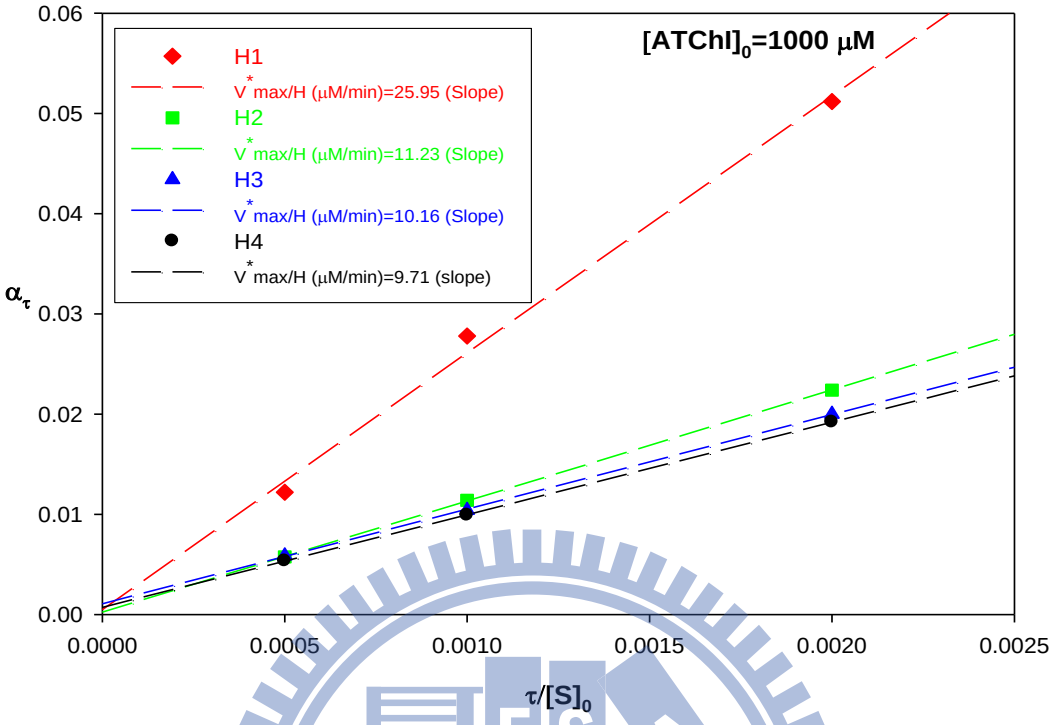

Figure 18. AChE kinetics. According to the second automatic program, the α_τ versus $\tau/[S]_o$ plot was used to determine initial V^*_{max}/H at high substrate concentration. Under saturating substrate condition, $[ATChI]_o$ = 1000 μM >> K_m, in the AChE assay, the slope of linear regression, V^*_{max}/H, were fitted to an exponential decay curve shown as the inset, which interpolated value was used to predict V^*_{max}/H at any time in the experimental intervals.

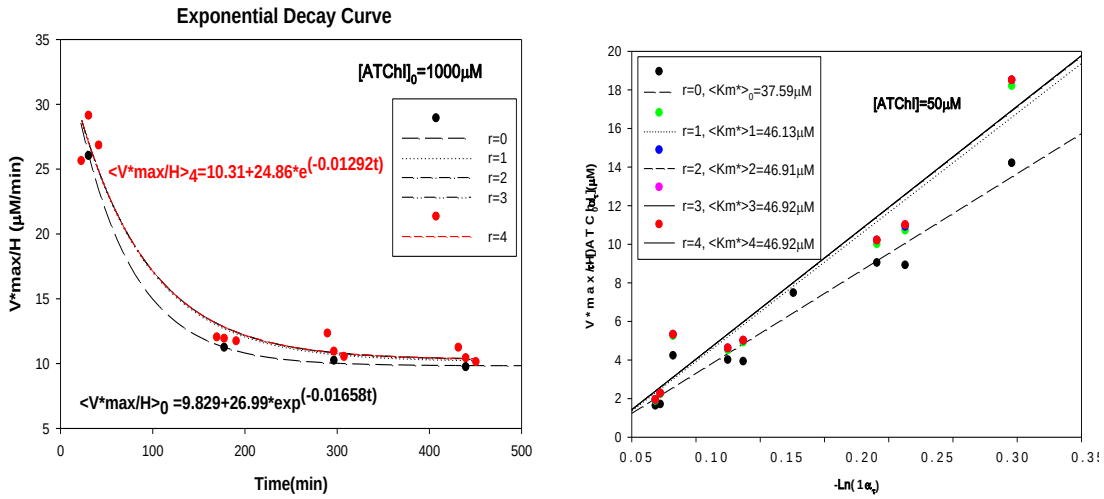

(a) (b)

Figure 19. AChE kinetics. The typical iterative plots (a) and (b) were the output values of the second and third automatic programs. (a) for the solubility limit of substrate $[ATChI]_o$ in the AChE assay, $[ATChI]_o$ = 1000 μM concentration used in this experiment, the initial approximation $<V^*_{max}/H>_0$ (black symbol) were still obtained from eq (2), and fitted to the exponential decay curve (r = 0). The r = 1~4 curves mean the fitting curves of five successive approximations of eq (1.3); the red symbol means the optimum value of V^*_{max}/H, which has converged to three significant figures. (b) The black symbol and red symbol mean the initial and the fourth approximations of eq (1.4), respectively. The value of K^*_m of immobilized AChE has converged to 46.92 μM after four successive approximation (r = 1~4).

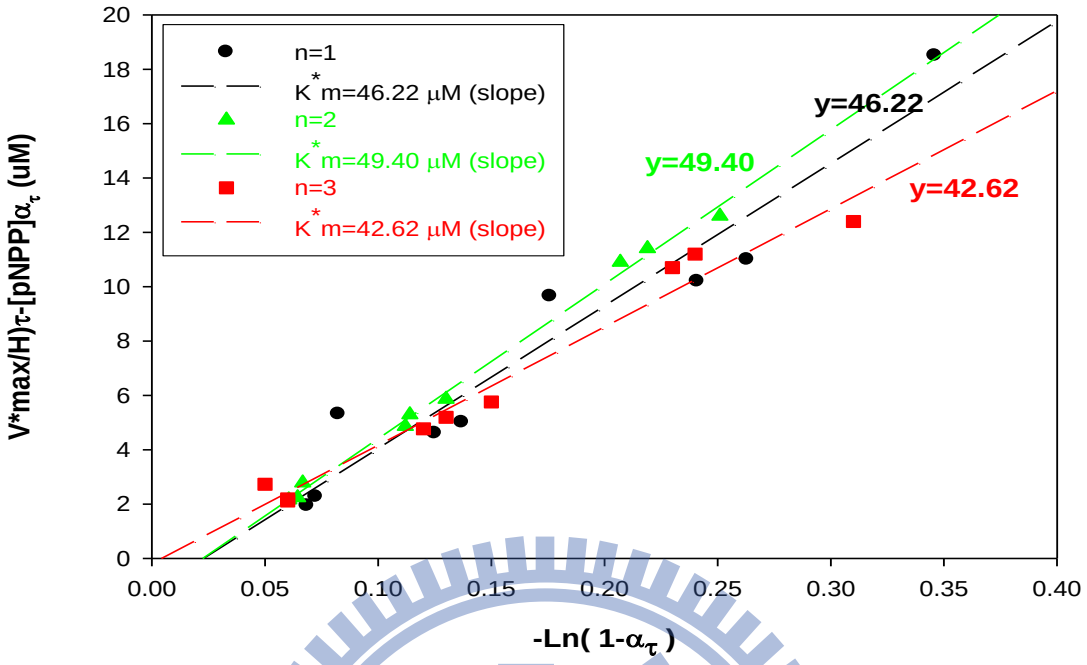

Figure 20. Kinetics of immobilized AChE. The predicted values of K^*_m of immobilized AChE are the result of three set of independent experiment data (n = 1~3).